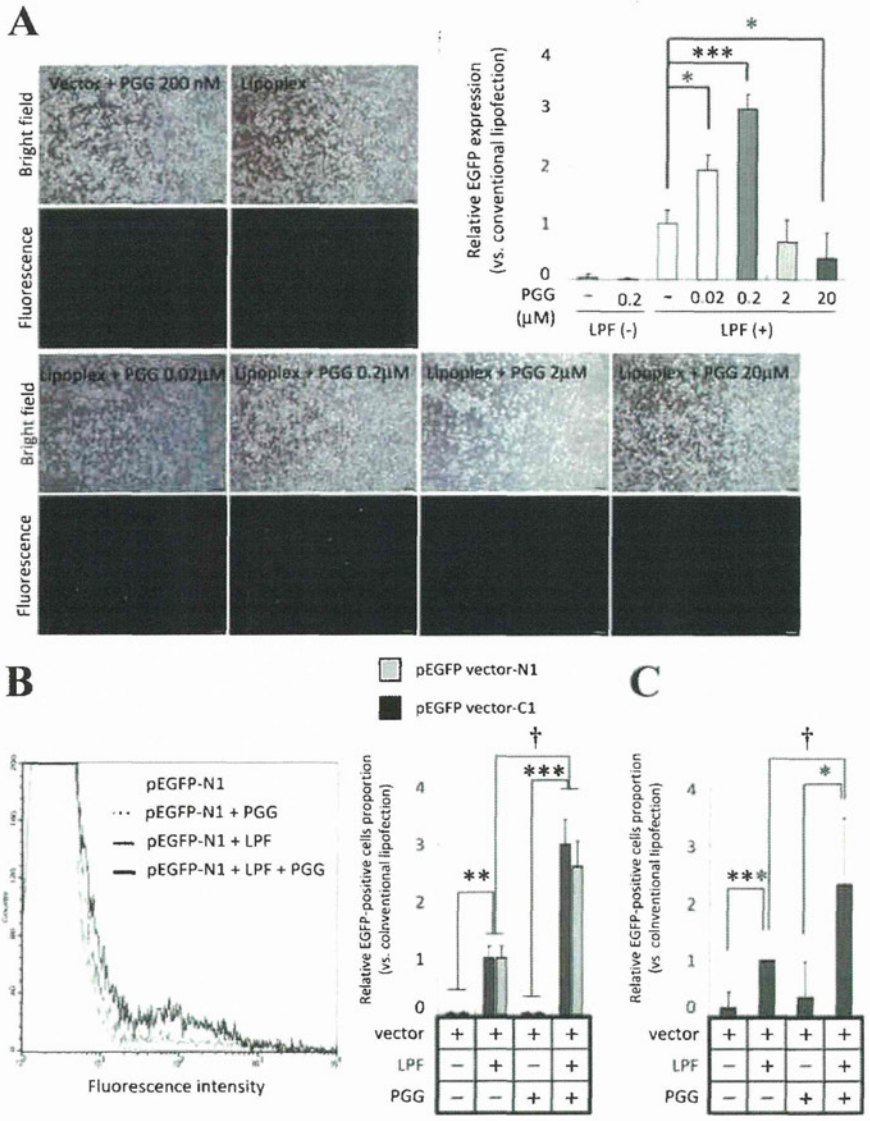

Fig. 2. Lipofection with Lipofectin (LPF) Combined with PGG in DC2.4 and Bone Marrow Derived Dendritic Cells

DC2.4 bone marrow derived dendritic cells were transfected with LPF and PGG together for 5 h. After 24 h of culture with growth medium at 37 °C, EGFP expression was obtained by fluorescence microscopy and flow cytometry. (A) Transfected DC2.4 cells with 2 μg pEGFP-N1 vector with 200 nM PGG (without Lipofection) (upper left), vector+LPF (lipoplex) (upper right), vector+LPF+PGG indicated concentration (lower panel). Up and downward square observe pictures under phase-contact microscopy and fluorescence image. Scale bar=100 μm. EGFP gene transduction of DC2.4 lipofected with indicated PGG concentration was expressed as EGFP expression (relative EGFP-positive cell proportion (fold)). (B) Histogram image shows EGFP intensity on DC2.4 cells transfected respectively. EGFP gene transduction of DC2.4 lipofected with indicated combination was expressed as EGFP expression (relative EGFP-positive cell proportion (fold)). (C) EGFP gene transduction of BMDCs lipofected with 4 μg pEGFP vector and indicated combination was expressed as EGFP expression (relative EGFP-positive cell proportion *vs.* conventional lipofection (fold)). Data are presented as the means±S.D. of (B) five or (C) three independent experiments. * $p<0.05$, ** $p<0.01$, *** $p<0.005$, *vs.* respective LPF-untreated group. † $p<0.01$, *vs.* PGG-untreated group by two-tail unpaired Student's *t*-test.

phagocytosis in the presence of LPF but the enhancement was lower than that of PGG. Additionally, GA also had a tendency to enhance phagocytosis, and the enhancement of GA was lower than that of TGG, suggesting that the ester binding mode between the glucose core and gallic acid rather than gallic acid itself is strongly involved in the enhancement of phagocytosis in DC2.4 cells (Fig. 1B).

Enhanced the Efficacy of Lipofection Using PGG in Mouse Dendritic Cells Gene transfer into DCs is critical for potential therapeutic applications as well as for study of the genetic basis of DC-mediated immunological development and immune regulation, however, transfection into DCs is difficult.[11] In particular, it is difficult to transduce naked or plasmid DNA on DCs.[9] The main advantages of lipofection are its ability to transfect all types of nucleic acids in a wide range of cell types, its ease of use, reproducibility and low toxicity,[16] therefore, development of more efficient lipofection must enable DC vaccine therapy, and knowledge of DCs biology should be disseminated.

Thus, we tested the effect of PGG on lipofection in DC2.4 cells because PGG enhanced phagocytic activity. In pilot studies of our lipofection, we determined the optimal concentrations of the transfection reagent, plasmid vector and the length of incubation required for the best expression of EGFP in DC2.4 cells. We basically performed lipofection according to the instructions of the manufactures using a GFP

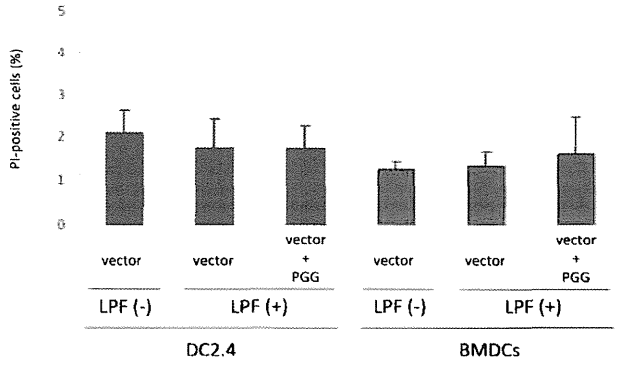

Fig. 3. Effect for Combination of Lipofectin (LPF) and 1,2,3,4,6-Penta-*O*-galloyl-β-D-glucose (PGG) in DC2.4 and BMDCs for Cell Viability

After 24 h of transfection, Propium iodide (PI) staining as DC2.4 and BMDCs viability was determined by flow cytometry. Data are presented as the means±S.D. of three independent experiments. No significant difference by ANOVA.

reporter construct, pEGFP-N1 and pEGFP-C1 vector to determine lipofection efficacy at 24 h posttransfection. For lipofection, we used 2 μg pEGFP-N1 or pEGFP-C1 vector as cytotoxicity (*i.e.*, cell detachment) was noted at higher amounts (data not shown) and 4 μl LPF. Lipofectin required an incubation period of >1 h with DC2.4 cells, whereas optimal results were obtained with about 5-h incubation in serum-free medium (EGFP-positive ($EGFP^+$) cells; 2.7±0.9%, $n=5$). Our lipofection efficacy corresponds to previous studies using lipofection in dendritic cells (lipofection efficacy is less than 2% or not detectable.).[9,41]

To evalutate the effect of PGG on lipofection, we used PGG in the preceding lipofection during incubation to prepare the pEGFP vector/LPF complex (lipoplex) for lipofection, and determined the efficacy of EGFP for lipofection efficacy by flow cytometry and fluorescent microscopy. PGG expectedly enhanced the expression of EGFP (Fig. 2) and enhancement was achived in a concentration-dependent manner, but more than 2 μM PGG did not enhance the expression of EGFP (Fig. 2A). Furthermore, DC2.4 cells transfected with pEGFP-N1 vector in combination with 200 nM PGG (without LPF) produced no detectable EGFP fluorescence. A similar phenomenon was also obtained for phagocytic activity in DC2.4 (Fig. 1). Hence, PGG synergistically enhanced phagocytosis and lipofection using LPF. A similar result was obtained using another vector, pEGFP-C1 (Fig. 2B). Thus, transfection activity in an immature dendritic cell line DC2.4 cells was highly enhanced by PGG.

To sophisticate and assess the function of PGG as an inducer of lipofection, we used bone marrow derived dendritic cells (BMDCs) instead of DC2.4 cells. BMDCs were evaluated by flowcytometer and phagocytic activity using FITC-dextran. BMDCs express both CD11c and MHC class II more than 70% of total population were used in our experiments and lipofection procedure on DC2.4 was also applied to BMDCs except for amount of plasmid vector, 2 μg plasmid vector changed to 4 μg. As a result, although the effect of PGG on lipofection efficacy in BMDCs did not seem to be strong, it was significantly enhanced (Fig. 2C). Therefore, PGG could enhance the lipofection efficacy in dendritic cell- or phagocytic cell-specific manner.

Effect of Lipofection with PGG on Dendritic Cells Viability In addition to measuring EGFP expression at 24 h posttransfection, we assessed the effect of lipofection combined with PGG on cell viability by staining with propium iodide (PI) and using a flow cytometer. In Fig. 3, DC2.4 and BMDCs were not damaged by lipofectin in combination with PGG, and 200 nM PGG by itself also did not exhibit cytotoxicity on these cells (determined using WST-1: cell proliferation assay; data not shown). PGG might not exhibit remarkable cytotoxicity because of the low concentration. Usually, non-viral transfections are harmful to DCs[9,17] and lipoplex can increase cytotoxicity along with lipofection efficacy in a dose-dependent manner.[42] Clinically, all vaccines and DNA-based DC vaccine therapies must be safe, therefore, PGG would be a useful aid for lipofection.

Does Lipofection in Combination with PGG Depend on Phagocytosis? We have suggested that PGG enhanced the effect of lipofection on DC2.4 cells and BMDCs, however, the action mechanism of PGG is still unclear. Although one possibility was shown that PGG enhanced phagocytic activity in DC2.4 cells (Fig. 1), it remained to be confirmed. PGG may also enhance lipofection efficacy by increasing phagocytic activity. In the next study, to determine whether the effect of PGG on lipofection depends on phagocytosis, we tested its effect using colon 26 cells, a murine colon carcinoma cell line. The endocytocytic lipoplex uptake pathway is further separated into phagocytosis (phagocytic cells) and pinocytosis (all cells).[43] As shown in Fig. 4, PGG slightly enhanced lipofection efficacy on colon 26 but not significantly, therefore, the enhancement of lipofection efficacy on DC2.4 and BMDCs by PGG greatly depend on intensified phagocytosis and is not implicated in the fusogenic effect. Namely, the effect of PGG would be restricted to phagocytic cells, like DCs.

The internalization mechanism of lipoplex is not well understood. An early report suggested that the fusogenic effect between the positively charged lipoplex and the plasma membrane is responsible for tranducing DNA into cytosol,[22] however, subsequent studies recently have shown the involvement of phagocytosis in delivering DNA.[44,45] Hence, it is currently believed along with this historical background that membrane fusion is important in lipofection but uptake of lipoplex largely depends on phagocytosis and endocytosis. According to our data, PGG specifically enhanced lipofection efficacy in DC2.4 cells and BMDCs. In other words, PGG enhanced some functions specifically found in DCs. Additionally, it was thought that phagocytosis facilitated by PGG enhanced lipofection efficacy.

A remaining question for our further study is which site of action of PGG is responsible for phagocytosis. In our lipofection protocol, PGG was added during the generation of lipoplex and transfection; namely, PGG affects lipoplex, DC2.4 or both to enhance lipofection efficacy.

If PGG modified lipoplex more effectively by making a lipoplex/PGG complex, PGG must enhance lipofection efficacy on colon 26 cells. It is unknown why they make a complex with each other, but the lipoplex/PGG complex must be phagocytosed through a DC-specific receptor. The recent identification of surface receptors expressed on DCs allow for a specific target for effective transfection.[46] Receptors such as FcγRI[47,48] and mannose[49,50] are attractive candidates for target cell surface molecules. If PGG has an affinity with

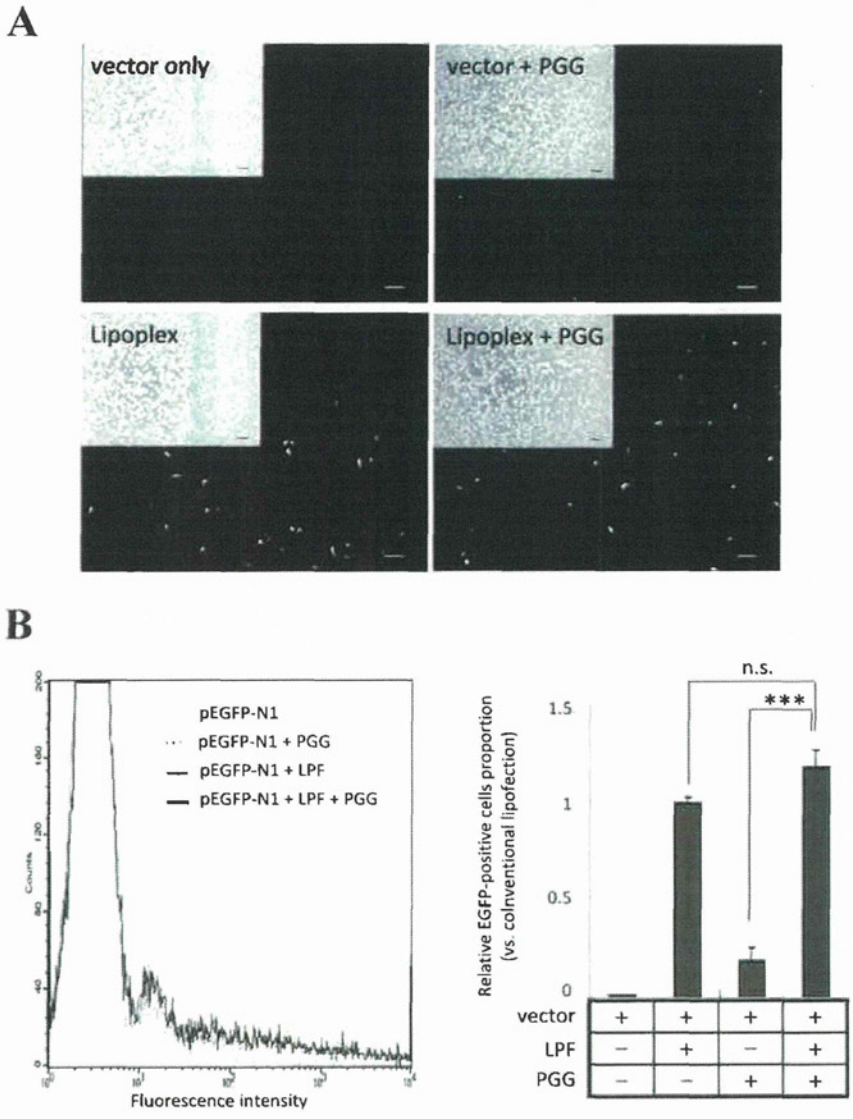

Fig. 4. Lipofection with Lipofectin (LPF) Combined with PGG in Colon 26

Colon 26 cells were transfected with LPF and PGG together. Lipofection and detection of EGFP used the same methods as for DC2.4 cells (*cf.* Fig. 2). (A) Transfected colon 26 with 2 μg pEGFP-N1 vector only (without Lipofection) (upper left), vector+200 nM PGG (upper right), vector+LPF (lower left), vector+LPF+200 nM PGG (lower right). Small squares show images under phase-contact microscopy. Scale bar=100 μm. (B) EGFP gene transduction of colon 26 lipofected with the indicated combination was expressed as EGFP expression (EGFP-positive cell proportion (%)). Data are presented as the means±S.D. of two or three independent experiments. *** $p<0.005$, *vs.* respective LPF-untreated group by two-tail unpaired Student's *t*-test. n.s.=no significant difference.

these cell surface receptors, the lipoplex/PGG complex may be easily phagocytosed. In previous studies, Li *et al.* reported that PGG binds to cell surface insulin receptor[51] and a number of researchers have studied the binding activity to biomolecules of PGG[29]; however it remains to be determined whether PGG binds to a DC-specific cell surface receptor. Furthermore, we have already suggested the importance of lipoplex incubation in combination with PGG for effective lipofection (data not shown). Consequently, we need to investigate the binding activity to cell surface receptor on DC2.4 cells and BMDCs in our further studies.

Secondly, we should focus on the DC maturation state if the action mechanism depends on the enhancement of phagocytosis. DCs have high phagocytic properties in the immature state, while few phagocytic properties in the mature state. Although DCs can phagocytose, they can be transformed by lipofection only with very low efficacy, perhaps due to their high nuclease content or easy of maturity by transfection. In this study, we used an immortalized murine immature DC line, DC2.4 cells[21] and primary immature BMDCs. These cells may be maturated by lipofection and lose phagocytic activity. As one possibility, PGG could maintain the phagocytic activity by inhibiting their maturation. DC maturation and differentiation are regulated by nuclear factor κB 2 (NF-κB2) and RelB, and these proteins are involved in vesicular transport.[52—54] Because previous reports have shown the inhibitory effect of PGG on NF-κB activity,[29,55] PGG probably maintaines an immature state by inhibiting a transcriptional factor, such as NF-κB. However, it has been reported that lipofectin alone or lipoplex could not induce maturation on DCs related to the cell surface expression of major histocompatibility (MHC) class I or II, CD40,

CD80, CD86, ICAM-I and IL-12 p40 expression,[33,34,53] and an inflammatory signal, LPS, was needed to change immature DCs into mature DCs.[56] Our phenotypical analysis of DC2.4 cells correspondingly demonstrated that cell surface expressions of MHC class II and CD80 were hardly increased by lipofection but were not inhibited by PGG (data not shown). Thus, we considered that PGG did not suppress DC maturation to maintain phagocytic activity.

Our data showed that PGG affected phagocytosis and lipofection efficacy in DC2.4 cells but the action mechanism has not been clarified. Hereafter, we must elucidate the mechanism in detail to understand DC biology and structure for a more highly effective lipofection method. If these challenges are achieved, DC vaccine therapy will develop markedly. Conventional DC vaccine therapies have already succeeded to some extent. In addition to these conventional therapies, DC vaccine therapy is expected to be highly effective and to be refined by more efficient lipofection of cytokines,[57] chemokines[58] and tumor-associated antigens (TAAs) using PGG.

Herbal medicine and medicinal plants have been used against a lot of diseases all over the world and considered enormous chemical library. Actually, various compounds have been found in medicinal plants, for example; resveratrol in grapes and the red wine prepared from them.[32] But, these reports showed only biological activities of medicinal plant-derived compounds. Our studies exhibit not only biological activities but also the pharmaceutical technological effectiveness as an application. Finally, our present findings provide an expectation that constituents from herbal plant enhance lipofection efficacy.

Acknowledgements This study was supported by a Grant for Health and Labour Sciences Research (H22-RINSHO KENKYU SUISHIN KENKYU-013 and SOUYAKU SOGO SUISHIN KENKYU-007) from the Ministry of Health Labour and Welfare, Japan. We thank Dr. N. Kageyama (Yahara) and Dr. M. Kadowaki, Division of Gastrointestinal Pathophysiology, Department of Bioscience, Institute of Natural Medicine, University of Toyama, for helpful advices and technical supports and Dr. N. Okada, Department of Biotechnology and Therapeutics, Graduate School of Pharmaceutical Sciences, Osaka University, for technical information and procedure about differentiation of BMDCs.

REFERENCES

1) Itano A. A., Jenkins M. K., *Nat. Immunol.*, **4**, 733—739 (2003).
2) Austyn J. M., *J. Exp. Med.*, **183**, 1287—1292 (1996).
3) Muriel M., Kenneth M. M., *Nat. Immunol.*, **1**, 199—205 (2000).
4) Falo L. D. Jr., Kovacsovics-Bankowski M., Thompson K., Rock K. L., *Nat. Med.*, **1**, 649—653 (1995).
5) Banchereau J., Palucka A. K., *Nat. Rev. Immunol.*, **5**, 296—306 (2005).
6) Gilboa E., *J. Clin. Invest.*, **117**, 1195—1203 (2007).
7) Nestle F. O., Farkas A., Conrad C., *Curr. Opin. Immunol.*, **17**, 163—169 (2005).
8) Okada N., Tsukada Y., Nakagawa S., Mizuguchi H., Mori K., Saito T., Fujita T., Yamamoto A., Hayakawa T., Mayumi T., *Biochem. Biophys. Res. Commun.*, **282**, 173—179 (2001).
9) Melhem N. M., Gleason S. M., Liu X. D., Barratt-Boyes S. M., *Clin. Vaccine Immunol.*, **15**, 1337—1344 (2008).
10) Larregina A. T., Morelli A. E., Tkacheva O., Erdos G., Donahue C., Watkins S. C., Thomson A. W., Falo L. D. Jr., *Blood*, **103**, 811—819 (2004).
11) Irvine A. S., Trinder P. K., Laughton, D. L., Ketteringham H., McDermott R. H., Reid S. C., Haines A. M., Amir A., Husain R., Doshi R., Young L. S., Mountain A., *Nat. Biotechnol.*, **18**, 1273—1278 (2001).
12) Flatz L., Hegazy A. N., Bergthaler A., Verschoor A., Claus C., Fernandez M., Gattinoni L., Johnson S., Kreppel F., Kochanek S., van den Broek M., Radbruch A., Lévy F., Lambert P., Siegrist C., Restifo N. P., Löhning M., Ochsenbein A. F., Nabel G. J., Pinschewer D. D., *Nat. Med.*, **16**, 339—345 (2010).
13) Engelmayer J., Larsson M., Subklewe M., Chahroudi A., Cox W. I., Steinman R. M., Bhardwaj N., *J. Immunol.*, **163**, 6762—6768 (1999).
14) Gao W., Rzewski A., Sun H., Robbins P. D., Gambotto A., *Biotechnol. Prog.*, **20**, 443—448 (2004).
15) Kavanagh D. G., Kaufmann D. E., Sunderji S., Frahm N., Gall S. L., Boczkowski D., Rosenberg E. S., Stone D. R., Johnston M. N., Wagner B. S., Zaman M. T., Brander C., Gilboa E., Walker B. D., Bhardwaj N., *Blood*, **107**, 1963—1969 (2006).
16) Felgner J. H., Kumar R., Sridhar C. N., Wheeler C. J., Tsai Y. J., Border R., Ramsey P., Martin M., Felgner P. L., *J. Biol. Chem.*, **269**, 2550—2561 (1994).
17) Rughetti A., Biffoni M., Sabbatucci M., Rahimi H., Pellicciotta I., Fattorossi A., Pierelli L., Scambia G., Lavitrano M., Frati L., Nuti M., *Gene Ther.*, **7**, 1458—1466 (2000).
18) Li G. B., Li G. X., *Mol. Biotechnol.*, **43**, 250—256 (2009).
19) Ohnishi Y., Fujii H., Hayakawa Y., Sakukawa R., Yamaura T., Sakamoto T., Tsukada K., Fujimaki M., Nunome S., Komatsu Y., Saiki I., *Cancer Sci.*, **89**, 206—213 (1998).
20) Matsuo M., Sakurai H., Koizumi K., Saiki I., *Cancer Lett.*, **251**, 288—295 (2007).
21) Shen Z., Reznikoff G., Dranoff G.,, Rock K. L., *J. Immunol.*, **158**, 2723—2730 (1997).
22) Felgner P. L., Gadek T. R., Holm M., Roman R., Chan H. W., Wenz M., Northrop J. P., Ringold G. M., Danielsen M., *Proc. Natl. Acad. Sci. U.S.A.*, **84**, 7413—7417 (1984).
23) Malone R. W., Felgner P. L., Verma I. M., *Proc. Natl. Acad. Sci. U.S.A.*, **86**, 6077—6081 (1989).
24) Debs R. J., Freedman L. P., Edmunds S., Gaensler K. L., Düzgünes N., Yamamoto K. R., *J. Biol. Chem.*, **265**, 10189—10192 (1990).
25) Chiang M. Y., Chan H., Zounes M. A., Freier S. M., Lima W. F., Bennett C. F., *J. Biol. Chem.*, **266**, 18162—18171 (1991).
26) Lin M. F., Davolio J., Garcia R., *Biochem. Biophys. Res. Commun.*, **192**, 413—419 (1993).
27) Lee S. J., Lee I. S., Mar W., *Arch. Pharm. Res.*, **26**, 832—839 (2003).
28) Genfa L., Jiang Z., Hong Z., Yimin Z., Liangxi W., Guo W., Ming H., Donglen J., Lizhao W., *Int. Immunopharmacol.*, **5**, 1007—1017 (2005).
29) Zhang J., Li L., Kim S. H., Hagermana A. E., Lü J., *Pharm. Res.*, **26**, 2066—2080 (2009).
30) Kaur G., Athar M., Alam M. S., *Chem. Biol. Interact.*, **171**, 272—282 (2008).
31) Toshkova R., Nikolova N., Ivanova E., Ivancheva S., Serkedjieva J., *Pharmazie*, **59**, 150—154 (2004).
32) Svajger U., Obermajer N., Jeras M., *Immunology*, **129**, 525—535 (2010).
33) Okada N., Saito T., Mori K., Masunaga Y., Fujii Y., Fujita J., Fujimoto K., Nakanishi T., Tanaka K., Nakagawa S., Mayumi T., Fujita T., Yamamoto A., *Biochim. Biophys. Acta-Gen. Subj.*, **1527**, 97—101 (2001).
34) Korsholm K. S., Agger E. M., Foged C., Christensen D., Dietrich J., Andersen C. S., Geisler C., Andersen P., *Immunology*, **121**, 216—226 (2007).
35) Elouahabi A., Ruysschaert J. M., *Mol. Ther.*, **11**, 336—347 (2005).
36) Lee S. M., Li M. L., Tse Y. C., Leung S. C., Lee M. M., Tsui S. K., Fung K. P., Lee C. Y., Waye M. M., *Life Sci.*, **71**, 2267—2277 (2002).
37) Rodriguez A., Regnault A., Kleijmeer M., Icciardi-Castagnoli P., Amigorena S., *Nat. Cell Biol.*, **1**, 362—368 (1999).
38) Luts M. B., Kukutsch N., Ogilvie A. L., Rössner S., Koch F., Romani N., Schuler G., *J. Immunol. Methods*, **223**, 77—92 (1999).
39) Haas J., Park E. C., Seed B., *Curr. Biol.*, **6**, 315—324 (1996).
40) Araki N., Johnson M. T., Swanson J. A., *J. Cell Biol.*, **135**, 1249—1260 (1996).
41) Van Tendeloo V. F., Ponsaerts P., Lardon F., Nijs G., Lenjou M., Van Broeckhoven C., Van Bockstaele D. R., Berneman Z. N., *Blood*, **98**, 49—56 (2001).

42) Nguyen L. T., Atobe K., Barichello J. M., Ishida T., Kiwada H., *Biol. Pharm. Bull.*, **30**, 751—757 (2007).
43) Khalil I. A., Kogure K., Akita H., Harashima H., *Pharmacol. Rev.*, **58**, 32—45 (2006).
44) Cotton M., Längle-Rouault F., Kirlappos H., Wagner E., Mechtler K., Zenke M., Beug H., Birnstiel M. L., *Proc. Natl. Acad. Sci. U.S.A.*, **87**, 4033—4037 (1990).
45) Friend D. S., Papahadjopoulos D., Debs R. J., *Biochim. Biophys. Acta–Biomembr.*, **1278**, 41—50 (1996).
46) Chikh G., Schutze-Redelmeir M. P., *Biosci. Rep.*, **22**, 339—353 (2002).
47) Serre K., Machy P., Grivel J. C., Jolly G., Brun N., Barbet J., Leserman L., *J. Immunol.*, **161**, 6059—6067 (1998).
48) Suzuki R., Utoguchi N., Kawamura K., Kadowaki N., Okada N., Takizawa T., Uchiyama T., Maruyama K., *Yakugaku Zasshi*, **127**, 301—306 (2007).
49) Sallusto F., Cella M., Danieli C., Lanzavecchia A., *J. Exp. Med.*, **182**, 389—400 (1995).
50) Diebold S. S., Plank C., Cotton M., Wagner E., Zenke M., *Somat. Cell Mol. Genet.*, **27**, 65—74 (2002).
51) Li Y., Kim J., Li J., Liu F., Liu X., Himmeldirk K., Ren Y., Wagner T. E., Chen X., *Biochem. Biophys. Res. Commun.*, **336**, 430—437 (2005).
52) Speirs K., Lieberman L., Caamano J., Hunter C. A., Scott P., *J. Immunol.*, **172**, 752—756 (2004).
53) Cejas P. J., Carlson L. M., Zhang J., Padmanabhan S., Kolonias D., Lindner I., Haley S., Boise L. H., Lee K. P., *J. Biol. Chem.*, **280**, 28412—28423 (2005).
54) Cejas P. J., Carlson L. M., Kolonias D., Zhang J., Lindner I., Billadeau D. D., Boise L. H., Lee K. P., *Moll. Cell. Biol.*, **25**, 7900—7916 (2005).
55) Pan M. H., Lin-Shiau S. Y., Ho C. T., Lin J. H., Lin J. K., *Biochem. Pharmacol.*, **59**, 357—367 (2000).
56) Tan P. H., Beutelspacher S. C., Wang Y. H., McClure M. O., Ritter M. A., Lombardi G., George A. J. T., *Mol. Ther.*, **11**, 790—800 (2005).
57) Curiel-Lewandrowski C., Mahnke K., Labeur M., Roters B., Schmidt W., Granstein R. D., Luger T. A., Schwarz T., Grabbe S., *J. Immunol.*, **163**, 174—183 (1999).
58) Nukiwa M., Andarini S., Zaini J., Xin H., Kanehira M., Suzuki T., Fukuhara T., Mizuguchi H., Hayakawa T., Saijo Y., Nukiwa T., Kikuchi T., *Eur. J. Immunol.*, **36**, 1019—1027 (2006).

nature COMMUNICATIONS

ARTICLE

Received 24 Sep 2011 | Accepted 8 Mar 2013 | Published 23 Apr 2013

DOI: 10.1038/ncomms2718 OPEN

Microbe-dependent CD11b$^+$ IgA$^+$ plasma cells mediate robust early-phase intestinal IgA responses in mice

Jun Kunisawa[1,2,3,4,5], Masashi Gohda[1,2], Eri Hashimoto[1], Izumi Ishikawa[1], Morio Higuchi[1,6], Yuji Suzuki[1], Yoshiyuki Goto[1,5,7], Casandra Panea[7], Ivaylo I. Ivanov[7], Risa Sumiya[1], Lamichhane Aayam[1,2], Taichi Wake[1,6], So Tajiri[1,2], Yosuke Kurashima[1,5,6], Shiori Shikata[1], Shizuo Akira[8], Kiyoshi Takeda[5,9] & Hiroshi Kiyono[1,2,3,5,6]

Intestinal plasma cells predominantly produce immunoglobulin (Ig) A, however, their functional diversity remains poorly characterized. Here we show that murine intestinal IgA plasma cells can be newly classified into two populations on the basis of CD11b expression, which cannot be discriminated by currently known criteria such as general plasma cell markers, B cell origin and T cell dependence. CD11b$^+$ IgA$^+$ plasma cells require the lymphoid structure of Peyer's patches, produce more IgA than CD11b$^-$ IgA$^+$ plasma cells, proliferate vigorously, and require microbial stimulation and IL-10 for their development and maintenance. These features allow CD11b$^+$ IgA$^+$ plasma cells to mediate early-phase antigen-specific intestinal IgA responses induced by oral immunization with protein antigen. These findings reveal the functional diversity of IgA$^+$ plasma cells in the murine intestine.

[1] Division of Mucosal Immunology, Department of Microbiology and Immunology, The Institute of Medical Science, The University of Tokyo, Tokyo 108-8639, Japan. [2] Department of Medical Genome Science, Graduate School of Frontier Science, The University of Tokyo, Chiba 277-8562, Japan. [3] International Research and Development Center for Mucosal Vaccines, The Institute of Medical Science, The University of Tokyo, Tokyo 108-8639, Japan. [4] Laboratory of Vaccine Materials, National Institute of Biomedical Innovation, Osaka 567-0085, Japan. [5] Core Research for Evolutional Science and Technology, Japan Science and Technology Agency, Tokyo 102-0075, Japan. [6] Graduate School of Medicine, The University of Tokyo, Tokyo 113-0033, Japan. [7] Department of Microbiology and Immunology, Columbia University Medical Center, New York, New York 10032, USA. [8] Laboratory of Host Defense, WPI Immunology Frontier Research Center, Osaka University, Osaka 565-0871, Japan. [9] Laboratory of Immune Regulation, Department of Microbiology and Immunology, Graduate School of Medicine, Osaka University, Osaka 565-0871, Japan. Correspondence and requests for materials should be addressed to J.K. (email: kunisawa@nibio.go.jp).

Immunoglobulin (Ig) A is an antibody found predominantly in the intestinal lumen, where it protects the host against pathogenic infections[1,2]. It also has an important role in the creation and maintenance of immunological homoeostasis by shaping homeostatic communities of commensal bacteria[3–5]. Indeed, some patients with IgA deficiency show marked susceptibility to infections with pathogens such as *Giardia lamblia*, *Campylobacter*, *Clostridium*, *Salmonella* and rotavirus; they also have increased incidences of intestinal immune diseases such as coeliac disease and inflammatory bowel diseases[6].

Peyer's patches (PPs) are the major sites for the initiation of antigen-specific intestinal IgA production, mainly in a T cell-dependent manner[7]. Intestinal IgA also originates from B1 cells. B1 cells differ from B2 cells in terms of origin, surface markers (for examples, B220, IgM, IgD, CD5, CD11b and CD23), growth properties and V_H repertoire[8–10]. B1 cells are predominantly present in the peritoneal cavity (PerC) and traffic into the intestinal compartment for the production of IgA against T cell-independent antigens such as DNA and phosphatidylcholine[11]. T cell independent antigen-specific IgA responses are also initiated in the isolated lymphoid follicles (ILFs), which are small clusters of B2 cells in the intestine[12].

Upon Ig class switching from μ to α, IgA^+ B cells acquire the expression of type 1 sphingosine-1-phosphate receptor, CCR9 and α4β7 integrin, allowing them to migrate out from the PPs or PerC and traffic to the intestinal lamina propria (iLP)[11,13,14]. In the iLP, they further differentiate into IgA-secreting plasma cells (PCs) under the influence of terminal differentiation factors (for example, IL-6)[15]. As these locally produced IgA antibodies are continuously transported and secreted by epithelial cells as a form of secretory IgA into the intestinal lumen, stably high levels of IgA production are required for the maintenance of sufficient amounts of IgA; this production is determined by the generation, survival and function of IgA PCs.

Several lines of evidence have demonstrated that the function and survival of PCs in the systemic compartments (for example, spleen and bone marrow (BM)) are not only determined by intrinsic factors but are regulated by the presence of environmental niches[16]. As with systemic PCs, differentiation of IgA PCs in the iLP is regulated by exogenous factors such as IgA-enhancing cytokines (for example, interleukin (IL)-5, IL-6, IL-10, IL-15, a proliferation-inducing ligand (APRIL) and B cell activating factor (BAFF))[7,15]. In addition, microbial stimulation is required for the full effects of intestinal IgA. Indeed, germ-free (GF) mice have decreased intestinal IgA responses with immature structures of PPs and ILFs[17,18]. Previous studies in mono-associated GF mice have indicated that only a small proportion of the total amount of intestinal IgA is reactive to monoassociated bacteria; microbe-dependent IgA production is therefore mediated by polyclonal stimulation through innate immune receptors such as toll-like receptors, rather than through B cell receptors specific for microbial antigens[19,20]. Accumulating evidence has revealed the molecular and cellular pathways of IgA production mediated by innate immunity, including the involvement of myeloid differentiation primary response gene 88 (MyD88) in the regulation of tumour necrosis factor/inducible nitric oxide synthase-producing DCs in the iLP[21] and follicular DCs in the PPs[22]. However, the effects of microbial stimulation on the regulation of differentiated IgA^+ PCs remain to be investigated. Here, we identified unique microbe-dependent subsets of IgA^+ PCs, which add a new level of complexity to the intestinal IgA system of mice.

Results

Microbe dependency of intestinal IgA^+ cells. To examine the immunological elements of intestinal IgA production associated with commensal bacteria, we initially compared the IgA^+ cells of specific pathogen-free (SPF) and GF mice. Flow cytometric analysis showed that $CD11b^+$ IgA^+ cells accounted for about 30% of IgA^+ cells, and we found a lack of $CD11b^+$ IgA^+ cells in the iLP of GF mice (Fig. 1a). Similarly, the numbers of intestinal $CD11b^+$ IgA^+ cells were reduced in both antibiotic-treated SPF mice and MyD88 KO mice (Fig. 1b–d). Immunohistological analysis indicated that $CD11b^+$ IgA^+ cells were dispersed throughout the iLP of wild-type (WT) mice (Fig. 1d), although their frequency appeared lower than expected from the flow cytometric data, probably because of difference in methodological sensitivity. These findings collectively suggest that $CD11b^+$ IgA^+ cells are unique subset that requires MyD88-dependent microbial stimulation for its development and maintenance.

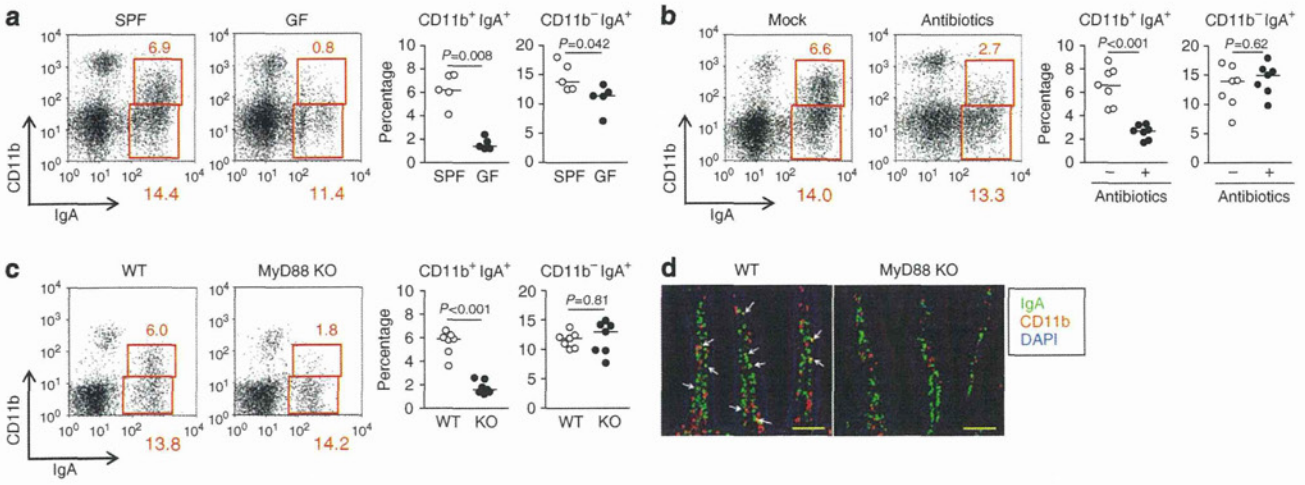

Figure 1 | Intestinal $CD11b^+$ IgA^+ cells require microbial stimulation. (**a**–**c**) Mononuclear cells were isolated from the small intestines of SPF or GF mice (**a**), mock- or antibiotic-treated SPF mice (**b**), or MyD88 WT or knockout (KO) mice (**c**) for analysis of IgA and CD11b expression by flow cytometry. Graphs show data from individual mice, and bars indicate median. Statistical analyses were performed with Mann–Whitney's *U*-test. (**d**) Specimens of small intestinal tissues of WT and MyD88 KO mice were stained for IgA and CD11b, and counterstained with 4′,6-diamidino-2-phenylindole. Data are representative of three independent experiments. Scale bars, 50 μm.

Intestinal CD11b$^+$ IgA$^+$ cells are PCs. We next aimed to characterize the CD11b$^+$ and CD11b$^-$ IgA$^+$ cells in the iLP. In addition to a gating strategy to exclude the possibility that the CD11b$^+$ IgA$^+$ cells detected by flow cytometry were doublets (Supplementary Fig. S1), we further performed a cytospin analysis and confirmed that both CD11b$^+$ and CD11b$^-$ IgA$^+$ cells had homogeneous morphology that was the same as that of PCs (for example, large irregular nuclei with prominent nucleoli), whereas CD11b^{hi} IgA$^-$ cells were composed of different kinds of cells, including eosinophils and macrophages (Fig. 2a). We also confirmed that both CD11b$^+$ and CD11b$^-$ IgA$^+$ cells did not express markers for macrophages (F4/80), DCs (CD11c) or eosinophils (CCR3) (Fig. 2b). Thus, CD11b$^+$ IgA$^+$ cells are neither doublets nor myeloid cells decorated by bound IgA on their surfaces.

CD11b$^+$ and CD11b$^-$ IgA$^+$ cells were identical in cell size and density, as determined by forward scatter (FSC) and side scatter (SSC), respectively, and by their surface expression patterns (CD19^{int}, B220$^-$, CD138$^+$, CD38^{hi} and CD40^{int}) (Fig. 2c). Although PCs in the systemic compartments (for example, the spleen) generally express little or no surface immunogloblin[23], we previously confirmed that CD38$^+$ CD138$^+$ cells in the iLP express IgA both on the cell surface and in the intracellular compartment (Supplementary Fig. S2)[13]. These findings indicated that both CD11b$^+$ and CD11b$^-$ IgA$^+$ cells could be classically categorized as PCs. This view was further supported by our finding that both populations expressed equal levels of Blimp1, a master transcription factor for PCs (Fig. 2c)[23].

The phenotypes of IgA$^+$ cells in the iLP differed from those of IgA$^+$ cells in the spleen. Splenic CD11b$^-$ IgA$^+$ cells exclusively had a memory phenotype (that is, B220$^+$, CD138$^-$, CD38^{int} and CD40^{hi}), whereas splenic CD11b$^+$ IgA$^+$ cells contained almost equal amounts of B220$^+$ CD138$^-$ CD38^{int} CD40^{hi} memory cells and B220$^-$ CD138$^+$ CD38^{hi} CD40^{low} PCs (Supplementary Fig. S3). These results indicated that CD11b$^+$ IgA$^+$ cells in the iLP were unique PCs that had an immunologically different status from splenic CD11b$^+$ IgA$^+$ cells.

Intestinal CD11b$^+$ IgA$^+$ PCs require PP lymphoid structure. CD11b$^+$ IgA$^+$ PCs expressed CD18 (Supplementary Fig. S4), which associates with CD11b and acts as a ligand for intercellular adhesion molecule-1 (ICAM-1)[24]. As ICAM-1 is an endothelial adhesion molecule that regulates cell trafficking[24,25], we considered that CD11b$^+$ IgA$^+$ PCs were recent emigrants from IgA-inductive tissues (for example, PPs and PerC) and had migrated into the iLP. To test this possibility, we employed FTY720 to inhibit the trafficking of IgA-committed B cells from PPs and PerC into the iLP. As we previously reported[11,13], FTY720 treatment reduced the numbers of intestinal IgA$^+$ PCs,

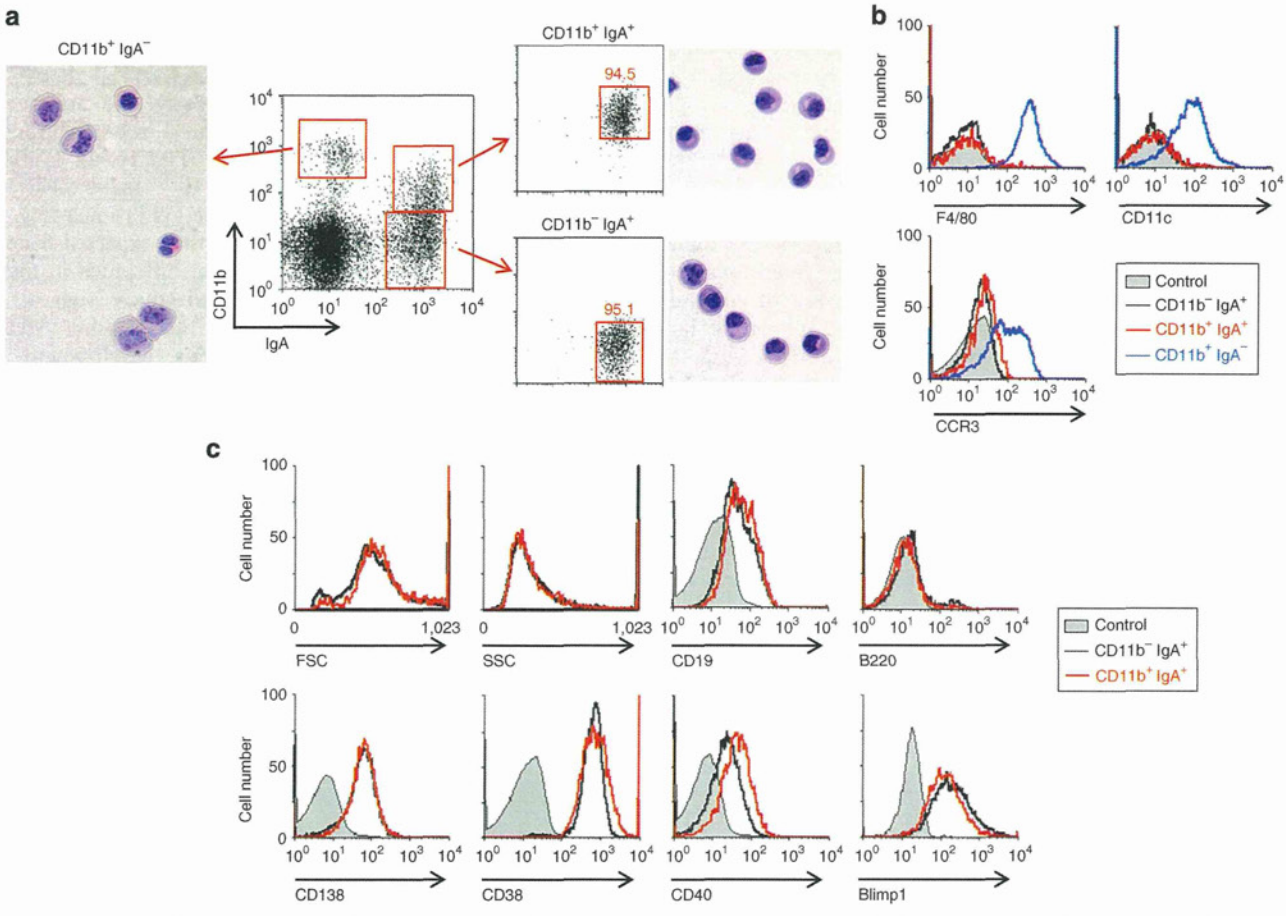

Figure 2 | Both CD11b$^+$ and CD11b$^-$ IgA$^+$ cells in the intestine are categorized as plasma cells. (**a**) Cells were purified by cell sorting from the iLP, and their morphology was examined by haematoxylin and eosin staining after cytospin. Data are representative of three independent experiments. (**b**) Cells were isolated from the iLP for the analysis of F4/80, CD11c and CCR3 expression on CD11b$^-$ IgA$^+$, CD11b$^+$ IgA$^+$ and CD11b$^+$ IgA$^-$ cells. Grey indicates isotype control. Similar results were obtained from three separate experiments. (**c**) Cells were isolated from the iLP for comparisons between CD11b$^+$ and CD11b$^-$ IgA$^+$ cells in terms of cell size (FSC) and density (SSC), and expression of CD19, B220, CD138, CD38, CD40 and Blimp1. Grey indicates isotype control. Similar results were obtained from five separate experiments.

but the effect was not specific to CD11b$^+$ IgA$^+$ PCs (Fig. 3a). These data suggested that CD11b$^+$ IgA$^+$ PCs were not recent emigrants from IgA inductive tissues (for example, PPs and PerC).

The second possibility was that CD11b$^+$ IgA$^+$ PCs originated from B1 cells, because CD11b is a marker of peritoneal B1 cells[26]. To test this possibility, peritoneal CD11b$^+$ B1 cells were purified and adoptively transferred into severe combined immunodeficiency mice. As we reported previously[11], adoptively transferred CD11b$^+$ B1 cells migrated into the intestine, where they differentiated into IgA$^+$ PCs. Although we transferred B cells expressing CD11b, they lost their CD11b expression in the iLP (Supplementary Fig. S5). Although only a few cells were detected in the iLP under these experimental conditions, CD11b expression was likely to be reversible on B cells and was thus not to be a marker of PCs originating from peritoneal CD11b$^+$ B1 cells.

As a third possibility for discriminating between CD11b$^+$ and CD11b$^-$ IgA$^+$ PCs, we examined the T cell dependency of their differentiation and IgA production. For this, we employed TCRβδ mice. Although TCRβ δ mice had decreased levels of intestinal IgA$^+$ cells, the ratio between CD11b$^+$ and CD11b$^-$ IgA$^+$ PCs did not differ between the WT mice and the TCRβ δ mice (Fig. 3b).

We also examined the production of IgA against T cell dependent and T cell independent antigens by CD11b$^+$ and CD11b$^-$ IgA$^+$ PCs. For the analysis of T cell dependent antigen, mice were orally immunized with ovalbumin (OVA) plus cholera toxin (CT). Following three oral immunizations, substantial amounts of OVA-specific IgA antibody-forming cells (AFCs) were detected in the iLP by enzyme-linked immunosorbent spot (ELISPOT) assay; this production was reduced by almost 50% when either the CD11b$^+$ IgA$^+$ or the CD11b$^-$ IgA$^+$ cells were removed before the ELISPOT assay (Fig. 3c). Similar results were obtained when we enumerated IgA AFCs against phosphorylcholine, a typical TI antigen, induced by commensal bacteria (Fig. 3c)[27]. These results collectively suggested that both CD11b$^+$ IgA$^+$ and CD11b$^-$ IgA$^+$ cells almost equally included IgA AFCs producing IgA antibodies specific for T cell dependent and T cell independent antigens.

Next, to examine the involvement of PPs, we established PP-null mice by *in utero* treatment with anti-IL-7Rα antibody[28] and found that PP-null mice had reduced numbers of CD11b$^+$ IgA$^+$ PCs in the iLP (Fig. 3d). In addition, CD11b was not expressed on IgA$^+$ B cells in the PPs (Fig. 3e). We treated mice with anti-IL-7Rα antibody only once *in utero* and confirmed that it did not affect the ILFs[28]. Although it is still possible that CD11b$^+$ IgA$^+$ PCs specifically require IL-7, the most plausible conclusion based on our current findings is that CD11b$^+$ IgA$^+$ B cells require the lymphoid structure of PPs, and CD11b$^-$ IgA$^+$ B cells acquire CD11b expression in the iLP.

As in antibiotic-treated and MyD88 KO mice (Fig. 1), the numbers of CD11b$^-$ IgA$^+$ PCs changed little in PP-null mice (Fig. 3d), suggesting that it is unlikely that CD11b$^+$ IgA$^+$ PCs differentiate back into CD11b$^-$ IgA$^+$ cells in the iLP. This view is further supported by the results of *in vitro* analysis. When purified CD11b$^+$ and CD11b$^-$ IgA$^+$ PCs were separately cultured with different kinds of stimulants (for example, phorbol 12-myristate 13-acetate plus ionomycin, or lipopolysaccharide) little change was noted in CD11b expression (Supplementary Fig. S6). Although the origin of these cells remains to be firmly established, it is plausible that CD11b$^+$ IgA$^+$ PCs act as a separate lineage once they differentiate in the iLP.

High proliferation activity of CD11b$^+$ IgA$^+$ PCs. We next performed a gene microarray analysis to assess the uniqueness of CD11b$^+$ IgA$^+$ PCs in the iLP. Gene ontology enrich-

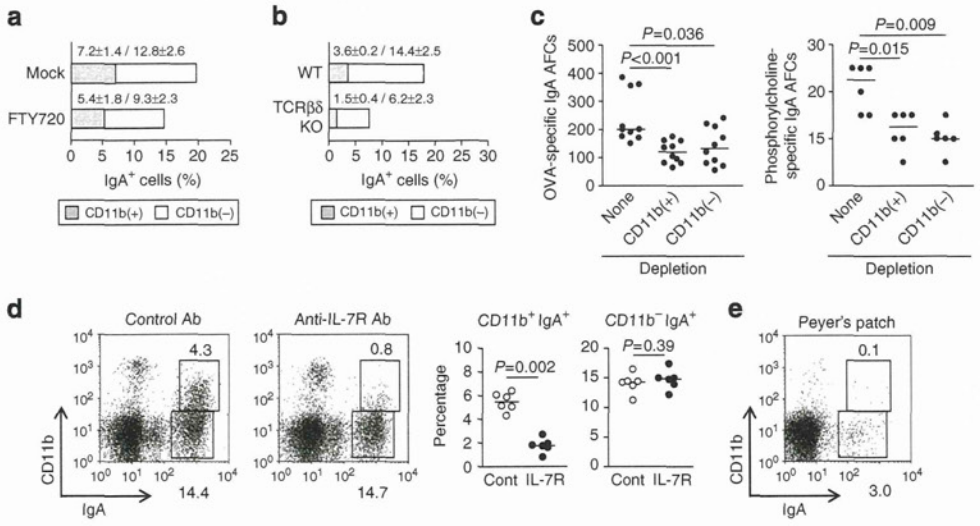

Figure 3 | CD11b$^+$ IgA$^+$ cells require the lymphoid structure of Peyer's patches. (**a**) Mice were treated with FTY720 every day for 5 days. The day after the final treatment, the proportions of CD11b$^+$ and CD11b$^-$ IgA$^+$ cells were measured by flow cytometry. Data are presented as means ± s.d. from four mice. Similar results were obtained from three separate experiments. (**b**) Proportions of CD11b$^+$ and CD11b$^-$ IgA$^+$ cells in the iLP of WT and TCRβδ KO mice were measured by flow cytometry. Data are presented as means ± s.d. from four mice. Similar results were obtained from three separate experiments. (**c**) After three oral immunizations with OVA plus cholera toxin, cells were isolated from the iLP and used in an ELISPOT assay to enumerate OVA-specific IgA AFCs. In some groups of mice, CD11b$^+$ or CD11b$^-$ IgA$^+$ cells were depleted by cell sorting before application of ELISPOT assay. Phosphorylcholine-specific IgA AFCs were measured. Graphs show data from individual mice, and bars indicate median. Statistical analyses were performed with Mann–Whitney's *U*-test. (**d**) Mononuclear cells were isolated from the iLP of Peyer's patch (PP)-normal (control Ab) and -null (anti-IL-7Rα Ab) mice for analysis of IgA and CD11b expression by flow cytometry. Graphs show data from individual mice. Statistical analyses were performed with Mann–Whitney's *U*-test. (**e**) Mononuclear cells were isolated from PPs for analysis of CD11b$^+$ and CD11b$^-$ IgA$^+$ cells by flow cytometry. Similar results were obtained from three separate experiments.

ment score computation analysis showed that the activity of cell-cycle-associated pathways was higher in CD11b$^+$ IgA$^+$ PCs than in CD11b$^-$ IgA$^+$ PCs (Supplementary Table S1). Consistent with this finding, higher expression of cell-cycle-associated genes was noted in CD11b$^+$ IgA$^+$ PCs than in CD11b$^-$ IgA$^+$ PCs; these genes included members of the cell division cycle family (Fig. 4a and Supplementary Table S2). In line with this, these cells expressed higher levels of the proliferation marker Ki67 than did CD11b$^-$ IgA$^+$ PCs (Fig. 4a and Supplementary Table S2). Additionally, CD11b$^+$ IgA$^+$ PCs showed greater uptake of bromodeoxyuridine (BrdU) than did CD11b$^-$ IgA$^+$ PCs (Fig. 4b). CD11b$^+$ IgA$^+$ PCs were preferentially removed by treatment with cyclophosphamide (CPM), which selectively targets proliferating cells (Fig. 4c). These data collectively suggested that CD11b$^+$ IgA$^+$ PCs possessed greater proliferating activity than did CD11b$^-$ IgA$^+$ PCs in the iLP.

Microarray analysis further identified CD150 (also known as signalling lymphocytic activation molecule family member 1, SLAMF1)[29], β1 integrin and CD168 (also known as hyaluronan-mediated motility receptor)[30] as possible candidates uniquely expressed on CD11b$^+$ IgA$^+$ PCs (Supplementary Table S3). Flow cytometric analysis confirmed that CD11b$^+$ IgA$^+$ PCs expressed higher levels of CD150 than did CD11b$^-$ IgA$^+$ PCs, whereas CD11b$^+$ IgA$^+$ and CD11b$^-$ IgA$^+$ PCs identically expressed β1 integrin and no CD168 (Supplementary Fig. S7).

IL-10 is essential for intestinal CD11b$^+$ IgA$^+$ cells. We next aimed to identify key molecules for inducing and maintaining CD11b$^+$ IgA$^+$ PCs in the iLP. As CD11b$^+$ IgA$^+$ PC numbers were reduced in MyD88 mice (Fig. 1c), and MyD88 is expressed in not only hematopoietic cells, including B cells, but also non-hematopoietic cells, including epithelial cells[31], we performed BM chimeric experiments to determine whether MyD88 in non-hematopoietic cells, hematopoietic cells, or both, was required for the generation of CD11b$^+$ IgA$^+$ cells. Similar levels of CD11b$^+$ IgA$^+$ cells were observed in irradiated WT mice receiving WT or MyD88 BM cells and in irradiated MyD88 mice receiving WT BM cells (Supplementary Fig. S8), suggesting that MyD88-dependent molecules commonly expressed in both non-hematopoietic and hematopoietic cells are involved in the microbe-dependent induction of CD11b$^+$ IgA$^+$ PCs.

We then examined the involvement of cytokines known to enhance IgA responses. Among several IgA-enhancing cytokines (for example, IL-5, IL-6, IL-10 and APRIL/BAFF)[7,15], we found that neutralization of IL-10 resulted in preferential reduction in CD11b$^+$ IgA$^+$ PCs, whereas blocking of other cytokines induced a reduction in IgA$^+$ cell numbers regardless of CD11b expression (Fig. 5a). Additionally, CD11b$^+$ IgA$^+$ cell numbers were preferentially reduced in IL-10 KO mice (Fig. 5b). As normal differentiation into IgA$^+$ B cells was observed in the PPs and PerC of IL-10 KO mice (Supplementary Fig. S9), it is plausible that IL-10 targets the maintenance of CD11b$^+$ IgA$^+$ cells in the iLP, but not the induction of IgA$^+$ cells in inductive tissues such as PPs and PerC.

Early-phase robust IgA responses by proliferating IgA$^+$ PCs. To examine the immunological importance of proliferating IgA$^+$ PCs present mainly in CD11b$^+$ IgA$^+$ PCs, mice were orally immunized with OVA plus CT. In this assay, one group received CPM treatment during immunization and the second group received CPM treatment 4 days after the final immunization (Fig. 6a). Because of the high cell-proliferation activity, CPM treatment during oral immunization resulted in efficient killing of peanut agglutinin (PNA^{hi}) B220$^+$ GC B cells and thus a reduction in the numbers of IgA$^+$ IgM$^-$ plasmablasts in the PPs (Supplementary Fig. S10). Thus, treatment with CPM during oral immunization led to an ~90% reduction in the numbers of OVA-specific IgA AFCs (Fig. 6b); this was associated with almost complete disappearance of faecal IgA produced against OVA (Fig. 6c). On the other hand, when mice were treated with CPM 4 days after the final immunization to remove proliferating cells mainly present in CD11b$^+$ IgA$^+$ cells in the iLP, the reduction in numbers of OVA-specific IgA AFCs in the iLP was only about 50% (Fig. 6b). This finding was consistent with our current finding that CD11b$^+$ IgA$^+$ PCs accounted for half the number of OVA-specific IgA AFCs (Fig. 3c). Thus, CPM treatment after the last immunization preferentially depleted CD11b$^+$ IgA$^+$ cells, with little influence on CD11b$^-$

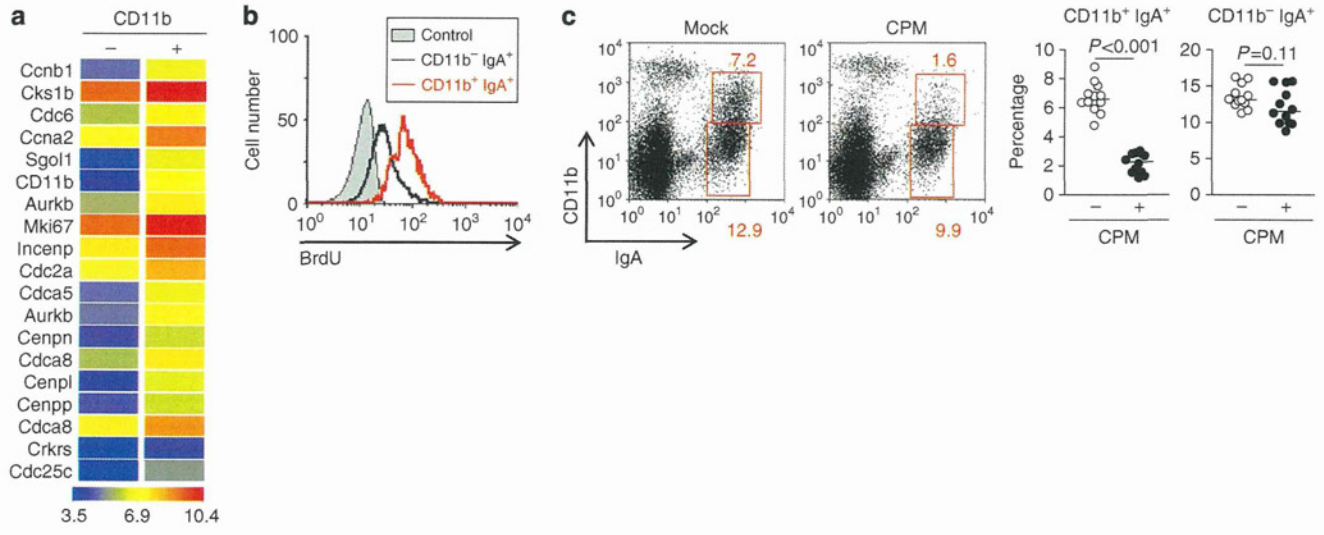

Figure 4 | CD11b$^+$ IgA$^+$ cells are proliferating cells. (**a**) mRNA was purified from small intestinal CD11b$^+$ and CD11b$^-$ IgA$^+$ cells and used for microarray analysis. Data related to the cell cycle and proliferation are shown. Data are representative of two independent experiments. (**b**) Mice were treated with BrdU, and uptake of BrdU by CD11b$^+$ and CD11b$^-$ IgA$^+$ cells was determined by flow cytometry. Data are representative of four independent experiments. (**c**) Cells were isolated from the intestinal lamina propria of mice receiving CPM to analyse CD11b$^+$ IgA$^+$ cells. Similar results were obtained from four separate experiments. Graphs show data from individual mice. Statistical analyses were performed with Mann-Whitney's *U*-test.

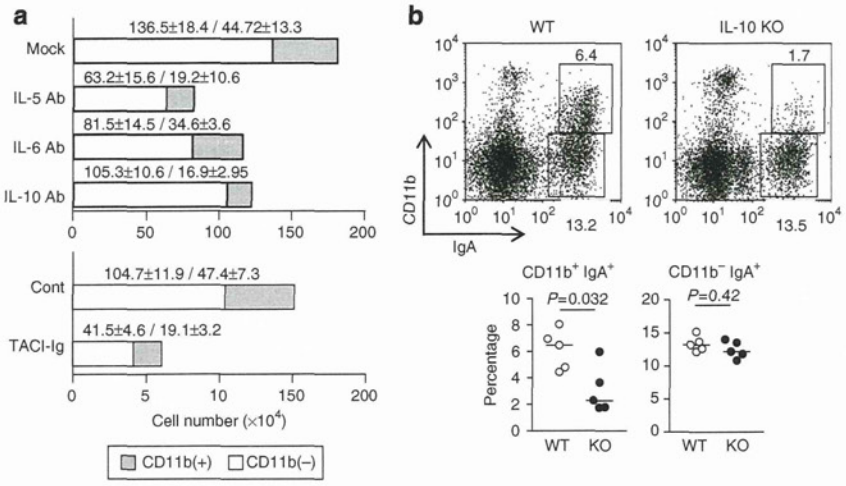

Figure 5 | Role of IL-10 in the maintenance of CD11b$^+$ IgA$^+$ cells in the iLP. (**a**) Mice were treated with antibodies to block IL-5, IL-6, IL-10 or antagonistic TACI-immunoglobulin (TACI-Ig) fusion protein. Mononuclear cells were isolated from the iLP and used for analysis of CD11b$^+$ and CD11b$^-$ IgA$^+$ cells by flow cytometry. Data are presented as means ± s.d. ($n=4$). (**b**) Mononuclear cells were isolated from the iLP of WT or IL-10 KO mice for analysis of IgA and CD11b expression by flow cytometry. Graphs show data from individual mice. Statistical analyses were performed with Mann–Whitney's *U*-test.

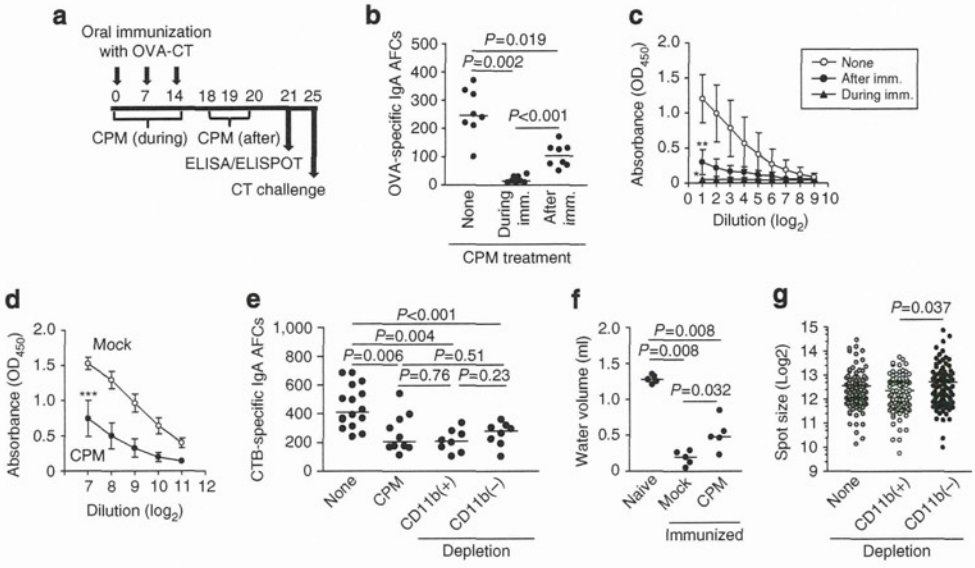

Figure 6 | Proliferating IgA$^+$ cells mediate early-phase IgA responses to oral antigen. (**a**) Experimental schedule for oral immunization and CPM treatment. Mice were orally immunized with OVA plus CT on days 0, 7 and 14. One group received CPM during oral immunization (days 0, 7 and 14) and another received CPM after the last immunization (days 18, 19 and 20). (**b**,**c**) One week after the final immunization (day 21), mononuclear cells were isolated from the iLP to quantify OVA-specific IgA-forming cells by ELISPOT (**b**). Simultaneously, faeces (**c**,**d**) were collected and were used for the detection of the (**c**) OVA-or (**d**) B subunit of CT (CTB)-specific IgA by enzyme-linked immunosorbent assay. Data are from individual mice and bars indicate median (**b**) and represent means ± s.d. ($n=10$) from two separate experiments (**c**,**d**). $^*P<0.001$, $^{**}P<0.01$, $^{***}P<0.05$ (two tailed unpaired *t*-test). (**e**) Mononuclear cells were isolated from the iLP of mock- or CPM-treated mice 1 week after the final immunization to quantify CTB-specific IgA-forming cells by ELISPOT. In some groups of mock-treated mice, CD11b$^+$ or CD11b$^-$ IgA$^+$ cells were depleted by cell sorting before application of ELISPOT assay. Graphs show data from individual mice, and bars indicate median. (**f**) On day 21, mice were orally challenged with 100 μg CT. After 15 h, the volume of intestinal fluid was measured. Graphs show data from individual mice, and bars indicate median. Similar results were obtained from two separate experiments. (**g**) Spot sizes of CTB-specific IgA AFCs were measured by Zeiss KS ELISPOT software. Graphs show data from individual mice, and bars indicate median. Statistical analyses were performed with Mann–Whitney's *U*-test (**e**–**g**).

IgA$^+$ cells. Of note, these mice showed ~90% reduction in OVA-specific IgA content in the faeces compared with mice not treated with CPM (Fig. 6c). We also confirmed that CPM treatment 4 days after final immunization induced a reduction in the production of IgA specific to the B subunit of CT (that is, CTB), which was associated with the halving of the abundance of CTB-specific IgA AFCs in the intestine (Fig. 6d,e). Like OVA-specific IgA responses (Figs. 3c and 6b), similar levels of reduction of CTB-specific IgA AFCs were noted when CD11b$^+$ IgA$^+$ cells were depleted before ELISPOT assay (Fig. 6e). These mice showed reduced resistance to oral challenge with CT and developed watery diarrhoea (Fig. 6f and Supplementary Fig. S11).

These findings led us to hypothesize that CD11b$^+$ IgA$^+$ PCs are capable of producing more IgA than are CD11b$^-$ IgA$^+$ PCs. To test this hypothesis, we measured the size of each spot in CTB-specific IgA AFCs in an ELISPOT assay. The cells in the CD11b$^+$ IgA$^+$ cell-enriched fraction (depletion of CD11b$^-$ IgA$^+$ cells) were bigger than those in the CD11b$^-$ IgA$^+$ cell-enriched fraction (depletion of CD11b$^+$ IgA$^+$ cells) (Fig. 6g). Furthermore, an adoptive transfer experiment demonstrated higher intestinal IgA production in severe combined immunodeficiency mice receiving CD11b$^+$ IgA$^+$ PCs than in those receiving CD11b$^-$ IgA$^+$ PCs (Supplementary Fig. S12), presumably because of both high IgA production and proliferating activity of CD11b$^+$ IgA$^+$ PCs. Although some possibilities (for example, proliferation and CD11b expression of IgA$^+$ cells might be changed during immunization) cannot be excluded, it is plausible that the actual production of IgA secreted into the intestinal lumen was derived mainly from CD11b$^+$ IgA$^+$ PCs in the early phase of the IgA response against orally immunized antigen.

Discussion

PCs could secrete antibodies to provide antigen-specific humoral immune responses in both systemic and mucosal tissues. Here, we demonstrated that intestinal IgA$^+$ PCs in mice could be categorized into two populations on the basis of CD11b expression. CD11b is an integrin αM that non-covalently associates with CD18 to form αMβ2 integrin (Mac-1) and binds to ICAM-1 (ref. 24). We therefore expected that CD11b$^+$ IgA$^+$ PCs were newly migrating cells whose migration was mediated by endothelial cells expressing ICAM-1, but in fact they were not. We also found no uptake of opsonized bacteria in either CD11b$^+$ or CD11b$^-$ IgA$^+$ cells (Supplementary Table S4 and Supplementary Fig. S13a), although CD11b is a receptor for complement (iC3b)[24]. In addition, unlike in human CD11b$^+$ B cells, which stimulate T cells strongly[32], major histocompatibility complex (MHC) class II (I-A^d) and costimulatory molecules (for example, CD80) were identically expressed on both CD11b$^+$ and CD11b$^-$ IgA$^+$ cells (Supplementary Table S4 and Supplementary Fig. S13b).

A similar subset of CD11b$^+$ IgA$^+$ cells was observed in the systemic murine compartments (for example, spleen), but the immunological characteristics of these cells differed from those of the cells in the intestine. Indeed, intestinal CD11b$^+$ IgA$^+$ cells consisted exclusively of PCs, but not memory B cells, whereas splenic CD11b$^+$ IgA$^+$ cells included both PCs and memory B cells. We further found that CD11b could not be used as a marker of B1 cells in the intestine. Our current findings show for the first time that CD11b could be a specific marker for discriminating IgA$^+$ PCs that require microbial stimulation and IL-10, and presumably contribute to the early phase of the intestinal IgA response in mice.

We have identified unique CD11b$^+$ IgA$^+$ PCs in mice; the next question is whether or not the same population of IgA$^+$ PCs exists in humans. Our preliminary experiments have shown that no human intestinal IgA$^+$ cells express CD11b, but that some IgA$^+$ cells express Ki67, a marker of proliferating cells (unpublished data). One possible explanation for this difference between human and mice is difference in the composition of commensal bacteria. In this regard, we examined the involvement of segmented filamentous bacteria (SFB), which are a known major IgA stimulus in mice, but has not yet been confirmed as part of the human microbiota[19]. As expected, SFB stimulated IgA production following colonization of SFB-deficient C57BL/6 mice from the Jackson laboratory (JAX mice) with bacterial suspensions from SFB-monoassociated mice (JAX + SFB mice)[33]; however, we found that CD11b is expressed on IgA$^+$ cells independently of SFB colonization (Supplementary Fig. S14). It is possible that other commensal bacteria such as *Lactobacillus* (abundant in mice) and *Bifidobacterium* (abundant in human) are responsible for the species-specific expression of CD11b on IgA$^+$ cells. It is important to recognize the differences between the mouse and human immune systems, but it is obvious that proliferating IgA$^+$ cells are present in the iLP of both mouse and human. The immunological function of human proliferating IgA$^+$ cells in the intestine will therefore be the subject of our next study.

In the initial step of the antibody response to T cell dependent antigens, B cells are activated by antigens and form GCs in the lymph nodes[7]. As depleting antigen-specific GC B cells by CPM treatment during oral immunization resulted in complete loss of the IgA response to orally immunized antigen, it is likely that both CD11b$^+$ and CD11b$^-$ IgA$^+$ PCs against T cell dependent antigen are derived from GC B cells. We also found that depletion of proliferating CD11b$^+$ IgA$^+$ PCs by CPM treatment after final immunization led to a decrease in the early-phase IgA response, although it is possible that proliferation activity and/or CD11b expression on IgA$^+$ cells might be wobble during immunization. Our *in vivo* findings indicated that the reduction in CD11b$^+$ IgA$^+$ PC numbers in MyD88 KO, IL-10 KO and PP-null mice did not affect the numbers of CD11b$^-$ IgA$^+$ PCs (Figs 1c, 3d and 5b). These findings, together with our *in vitro* data (Supplementary Fig. S6), indicate that it is likely that CD11b$^+$ IgA$^+$ PCs act as a separate lineage once they differentiate in the iLP.

Proliferating CD11b$^+$ IgA$^+$ PCs required microbial stimulation in the intestine. As proliferation is one of the characteristics of plasmablasts, it was possible that CD11b$^+$ IgA$^+$ cells have been recently committed to the PC fate. Notably, intestinal IgA$^+$ cells expressed MHC class II molecules; this expression is one of the unique characteristics of plasmablasts. Therefore, it is likely that intestinal IgA$^+$ PCs partly retain their plasmablast features. However, our findings indicated that CD11b$^+$ and CD11b$^-$ IgA$^+$ cells expressed identical levels of Blimp-1 and MHC class II. In addition, similar reduction was noted in CD11b$^+$ and CD11b$^-$ IgA$^+$ cells when cell trafficking from IgA inductive tissues (for example, PPs and the PerC) into the iLP was inhibited by treatment with FTY720. Thus, our findings suggest that CD11b$^+$ IgA$^+$ cells uniquely exhibit high proliferating and IgA-producing activity, although their other immunological features as PCs are similar to those of CD11b$^-$ IgA$^+$ PCs.

Proliferating CD138$^+$ PCs have been detected in the spleens of NZB/W mice with signs of systemic lupus erythematosus, but not in naive mice[34]. In contrast, the number of non-proliferating CD138$^+$ PCs is unchanged in the intestines of GF mice, as it is in the spleens of NZB/W mice[34]. These findings suggest that MyD88-dependent homeostatic stimulation of commensal bacteria determines the fate of proliferating CD11b$^+$ IgA$^+$ CD138$^+$ PCs in the intestine. Several lines of evidence have revealed the cellular and molecular mechanisms of microbe-dependent initiation of IgA responses. B cells express several toll-like receptors, and B cell-intrinsic MyD88-mediated signalling has been implicated in enhanced antibody production in some studies[35,36]. However, our current findings indicated that MyD88-mediated signalling in hematopoietic cells, including B cells, was not essential for intestinal CD11b$^+$ IgA$^+$ PC production. Additionally, we found IL-10 as a key molecule inducing CD11b$^+$ IgA$^+$ PC production. Previous studies have demonstrated that IL-10 promotes the proliferation of activated B cells and subsequent IgA production *in vitro*[37,38], which are consistent with our current findings of high-level proliferation of, and IgA production by, CD11b$^+$ IgA$^+$ PCs. Thus, our current findings proved that IL-10 functions in IgA production *in vivo* and that CD11b$^+$ IgA$^+$ PCs are the main targets in this

pathway. Despite these findings, our preliminary study demonstrated that treatment of $CD11b^+$ or $CD11b^-$ IgA^+ PCs with IL-10 alone did not induce their reciprocal differentiation into each other, and IL-10 KO mice with colitis possessed $CD11b^+$ IgA^+ PCs (J.K., unpublished data). Thus, IL-10 is redundant in some cases and additional factors are required for the maintenance of $CD11b^+$ IgA^+ PCs. Our current findings identified CD150 as a surface molecule that is highly expressed on $CD11b^+$ IgA^+ PCs. CD150 is a 70-kDa glycoprotein expressed on some B and T cells, thymocytes and macrophages[29]. Homophilic interaction of CD150 induces proliferation of, and antibody synthesis by, B cells[39], and notably IL-10 synergistically enhances CD150-mediated B cell proliferation[39]. Thus, it is likely that, at least partly, IL-10 and CD150 determine the unique features (for example, proliferation and high IgA production) of $CD11b^+$ IgA^+ PCs in the iLP. In addition, accumulating evidence has revealed an important immunological function of stromal cells as survival niches for PCs in the BM[40] and intestine[41,42]. It is possible that complex immunological communications among commensal flora, epithelial and stromal cells, and the cells involved in innate and acquired immunity determine the differentiation and maintenance of IgA PCs in the intestine.

Taken together, our results provide new insights into the nature of IgA^+ PCs in the murine intestine, and especially into the regulation of the early-phase IgA responses to intestinal antigens and requirement of microbe-dependent stimulation, IL-10, and the PP lymphoid structure. These findings add a new level of complexity to the intestinal IgA system of mice.

Methods

Mice. SPF and GF Balb/c mice were obtained from Japan CLEA (Tokyo, Japan). MyD88 KO mice, IL-10 mice (Balb/c background) and TCRβδ mice (C57/BL6 background) were maintained under SPF conditions at the Experimental Animal Facility, The Institute of Medical Science, The University of Tokyo, and WT littermates were used as controls. To deplete gut commensal bacteria, mice received broad-spectrum antibiotics, namely ampicillin (1 g l^{-1}; Sigma-Aldrich, St Louis, MO), vancomycin (500 mg l^{-1}; Shionogi, Osaka, Japan), neomycin sulphate (1 g l^{-1}; Sigma-Aldrich) and metronidazole (1 g l^{-1}; Sigma-Aldrich), in their drinking water for 4 weeks[43]. To establish BM chimeric mice, we injected γ-irradiated (960 rad, Gammacell 40, Atomic Energy of Canada Limited, Ontario, Canada) recipient mice with 5×10^6 BM cells through the tail vein and used them in experiments 8 weeks after injection. Under our experimental conditions, the reconstitution efficacy was about 90–95%. To obtain PP-null mice, pregnant BALB/c mice were injected intravenously and subcutaneously with 1 mg anti-IL-7Rα antibody (A7R34, BioLegend, San Diego, CA) at 14.5 days post coitus, as described previously[28]. We confirmed the disruption of organized PPs and the existence of ILFs in the offspring, as described previously[28]. To neutralize cytokines, mice were treated intraperitoneally with 250 μg of monoclonal antibodies specific for IL-5 (TRFK5), IL-6 receptor (D7715A7) or IL-10 (JES5.16E3) (BioLegend, San Diego, CA); control antibody (Rat IgG2b); or 100 μg of soluble TACI-Fc fusion protein (R&D Systems, Minneapolis, MN) every second day for 2 weeks[44,45]. For assessing the role of SFB, mice purchased from the Jackson laboratory were orally inoculated with bacterial suspensions obtained by homogenizing faecal pellets from SFB-monoassociated mice in water. SFB colonization was confirmed by quantitative PCR[33] and $CD11b^+$ IgA^+ cells were analysed in the small intestine 2 weeks post gavage by flow cytometry. All experiments followed the guidelines of the Animal Care and Use Committee, The University of Tokyo and Columbia University.

Oral immunization. Mice were given sodium bicarbonate solution to neutralize stomach acid[11,13]. Thirty minutes later, the mice were orally immunized with 1 mg OVA (Sigma-Aldrich) and 10 μg CT (List Biological Laboratories, Campbell, CA). This procedure was conducted on days 0, 7 and 14. In some groups, mice were intraperitoneally given CPM (35 mg kg^{-1} each time, Sigma-Aldrich). One week after the final immunization, faecal samples and mononuclear cells from the iLP were collected for enumeration of OVA-specific antibody responses by enzyme-linked immunosorbent assay and ELISPOT, respectively[13]. *In vivo* CT challenge was performed by oral challenge of naive or immunized mice with 100 μg of CT as previously described[46].

Cell isolation. To isolate mononuclear cells from PPs, we stirred the tissues in RPMI-1640 medium containing 2% fetal calf serum plus 0.5 mg ml^{-1} collagenase (Wako, Osaka, Japan)[11,13]. To isolate mononuclear cells from the iLP, PPs were carefully removed and the remaining intestines including ILFs were opened longitudinally, washed with RPMI-1640, cut into 2-cm pieces and stirred for 20 min at 37 °C into RPMI-1640 containing 0.5 mM EDTA and 2% fetal calf serum to remove epithelial cells and intraepithelial lymphocytes[11,13]. The tissues were then stirred three times in 0.5 mg ml^{-1} collagenase for 20 min before undergoing discontinuous Percoll gradient centrifugation (40 and 75%). Peritoneal cells were obtained by peritoneal flushing with 8 ml ice-cold phosphate-buffered saline (PBS)[11,13].

Flow cytometry and cell sorting. Mononuclear cells were preincubated with 10 μg ml^{-1} anti-CD16/32 antibody (BD Biosciences, San Diego, CA). They were then reacted with the following antibodies: Pacific blue-rat anti-mouse CD45R (B220) (RA3-6B2, 0.8 μg ml^{-1}), phycoerythrin (PE)-rat anti-mouse CD11b (M1/70, 0.1 μg ml^{-1}), PE-Cy7-hamster anti-mouse CD11c (HL3, 0.4 μg ml^{-1}), PE-rat anti-mouse CD18 (C71/16, 0.8 μg ml^{-1}), PE-rat anti-mouse CD19 (1D3, 0.8 μg ml^{-1}), PE-rat anti-mouse CD38 (90, 0.13 μg ml^{-1}), FITC-rat anti-mouse IgA (C10-3, 2 μg ml^{-1}), PE-Cy7-rat anti-mouse IgM (R6-60.2, 1 μg ml^{-1}), PE-anti-mouse $I\text{-}A^d$ (AMS-32.1, 0.4 μg ml^{-1}), APC-Cy7-rat anti-mouse CD11b (M1/70, 1 μg ml^{-1}), APC-Cy7-anti-mouse β1-integrin (HMβ1-1, 4 μg ml^{-1}), APC-anti-mouse CD40 (3/23, 2 μg ml^{-1}), Pacific blue-anti-mouse CD11b (M1/70, 1 μg ml^{-1}), PE-Cy7-anti-mouse F4/80 (BM8, 0.4 μg ml^{-1}) and biotin mouse anti-CD138 (281-2, 10 μg ml^{-1}) (all antibodies from BD Biosciences) followed by incubation with streptavidin-APC (1 μg ml^{-1}, BD Biosciences), PE-anti-mouse CD150 (TC15-12F12.2, 0.1 μg ml^{-1}), Alexa Fluor 647-anti-mouse CD80 (16-10A1, 1 μg ml^{-1}) (BioLegend, San Diego, CA), anti-mouse CD267 (TACI) (8F10-3, 4 μg ml^{-1}) (eBioscience, San Diego, CA), PE-mouse CCR3 (83101, 0.5 μg ml^{-1}) (R&D Systems) or biotinylated anti-peanut agglutinin lectin (1 μg ml^{-1}, Vector Laboratories, Burlingame, CA), followed by staining with streptavidin PE (1 μg ml^{-1}, BD Biosciences). For staining for Blimp-1, cells were fixed and permeabilized with a Cytofix/Cytoperm kit (BD Biosciences) and stained with PE-conjugated anti-Blimp1 goat polyclonal IgG (0.4 μg ml^{-1}, Santa Cruz Biotechnology, Santa Cruz, CA). FSC-H and FSC-A discrimination was used to exclude doublet cells, and ViaProbe cell-viability solution (BD Biosciences) was used to discriminate between dead and living cells. To detect proliferating cells, mice received 1 mg BrdU intraperitoneally 24 h before analysis; the BrdU signal was detected with the manufacturer's protocol (BD Biosciences). Concentration-matched isotype antibodies were used as negative controls. Flow-cytometric analysis and cell sorting were performed with FACSCanto II and FACSAria (BD Biosciences), respectively. We confirmed that cell purity was about 95% (Fig. 2a).

Immunohistological analysis. Intestines were fixed in 4% paraformaldehyde for 15 h at 4 °C, washed with PBS and treated sequentially in 10 and 20% sucrose for 12 h at 4 °C[13]. The tissues were embedded in OCT compound (Sakura Finetechnical Co., Tokyo, Japan). Cryostat sections (7 μm) were pre-blocked with anti-CD16 and CD32 antibody for 15 min at room temperature and stained for 15 h at 4 °C with FITC-rat anti-mouse IgA (C10-3, 2 μg ml^{-1}) and biotin anti-mouse CD11b antibody (M1/70, 1 μg ml^{-1}). This was followed by incubation with horseradish peroxidase (HRP)-conjugated streptavidin (Pierce, Rockford, IL) for 30 min at 4 °C and amplification of the fluorescent signal with Cy3-tyramide (TSA-Direct kit; PerkinElmer, Waltham, MA)[13]. We confirmed that no signal was detected when the specimens were stained with the concentration-matched isotype antibodies. They were then counterstained with 4′,6-diamidino-2-phenylindole (Sigma-Aldrich). Deconvoluted fluorescence images of specimens were obtained by fluorescence microscopy (BZ9000, Keyence, Osaka, Japan).

Detection of antibody responses by enzyme-linked immunosorbent assay and ELISPOT. To measure OVA- or CTB-specific IgA levels in faecal extracts, faeces were homogenized in PBS by vigorous vortexing[11,13]. After centrifugation of the extracts (9,000*g* for 15 min) the supernatants were used as faecal extracts. Plates were coated with 1 mg ml^{-1} OVA or 2 μg ml^{-1} CTB in PBS; this was followed by blocking for 1 h at room temperature with 200 μl PBS containing 1% (w/v) bovine serum albumin. After extensive washing of the plates with PBS containing 0.05% Tween 20, serial sample dilutions were added for incubation overnight at 4 °C. Samples were then incubated for 1 h at room temperature with optimally diluted HRP-conjugated goat anti-mouse IgA (SouthernBiotech, Birmingham, AL). After sample washing, the colour reaction was developed at room temperature with 3,3′,5,5′-tetramethylbenzidine (Moss, Pasadena, MD) and terminated by adding 0.5 M HCl. The colour reaction was measured as the optical density (wavelength 450 nm).

ELISPOT assay was used to enumerate IgA-producing AFCs in the iLP[11,13]. Briefly, various concentrations of mononuclear cells were cultured at 37 °C for 4 h in 96-well nitrocellulose membrane plates (Millititer HA; Millipore, Bedford, MA) coated with 1 mg ml^{-1} OVA and 5 μg ml^{-1} bovine serum albumin-conjugated phosphorylcholine (Biosearch Technologies, Novato, CA). After vigorous washing of the plates with PBS and PBS containing 0.05% Tween 20, HRP-conjugated goat anti-mouse IgA was added; the plates were then incubated overnight at 4 °C. Spots of AFCs were developed with 2-amino-9-ethylcarbazole

(Polysciences, Warrington, PA). The size of each spot was measured with Zeiss KS ELISPOT software (Oberkochen, Germany).

***In vitro* culture**. CD11b$^+$ IgA$^+$ or CD11b$^-$ IgA$^+$ PCs (10^4 cells per well) were purified from the iLP and cultured with 100 ng ml^{-1} phorbol 12-myristate 13-acetate plus 300 ng ml^{-1} ionomycin, or 10 μg ml^{-1} lipopolysaccharide (all from Sigma-Aldrich), for 24 h.

For the bacteria uptake assay, fluorescent *Staphylococcus aureus* was opsonized in accordance with the manufacturer's protocol (Molecular Probes). Mononuclear cells isolated from the iLP (2×10^5 cells) were incubated with 1×10^5 opsonized bacteria for 90 min. After being washed, the cells were stained with antibodies for PE-IgA (mA-6E1, 0.5 μg ml^{-1}, eBioscience) and Pacific Blue CD11b, and the bacterial uptake by each population was examined by flow cytometry.

Microarray analysis. Microarray analysis was performed as we previously reported[47]. Briefly, CD11b$^+$ IgA$^+$ and CD11b$^-$ IgA$^+$ cells were isolated from the iLP, and total RNA was extracted from them with an RNeasy kit (Qiagen, Dusseldorf, Germany). cRNA was hybridized with DNA probes on a GeneChip Mouse Genome 430 2.0 array (Affymetrix), washed and fluorescence-labelled in accordance with the standard amplification protocol developed by Affymetrix. The fluorescence intensity of each probe was taken to represent the raw expression level and was quantified with GeneChip Operating software (Affymetrix). Data obtained from two independent experiments were analysed with GeneSpring 7.3.1 software (Silicon Genetics). All microarray data have been deposited in the National Center for Biotechnology Information Gene Expression Omnibus database (www.ncbi.nlm.nih.gov/geo/) under the accession no. GSE37225.

Statistics. Results were compared by a non-parametric Mann–Whitney's *U*-test and unpaired *t*-test (two tailed) (GraphPad Software, San Diego, CA).

References

1. Macpherson, A. J., McCoy, K. D., Johansen, F. E. & Brandtzaeg, P. The immune geography of IgA induction and function. *Mucosal Immunol.* **1,** 11–22 (2008).
2. Brandtzaeg, P. Function of mucosa-associated lymphoid tissue in antibody formation. *Immunol. Invest.* **39,** 303–355 (2010).
3. Fagarasan, S. Intestinal IgA synthesis: a primitive form of adaptive immunity that regulates microbial communities in the gut. *Curr. Top Microbiol. Immunol.* **308,** 137–153 (2006).
4. Macpherson, A. J. & Slack, E. The functional interactions of commensal bacteria with intestinal secretory IgA. *Curr. Opin. Gastroenterol.* **23,** 673–678 (2007).
5. Slack, E. *et al.* Innate and adaptive immunity cooperate flexibly to maintain host-microbiota mutualism. *Science* **325,** 617–620 (2009).
6. Woof, J. M. & Kerr, M. A. The function of immunoglobulin A in immunity. *J. Pathol.* **208,** 270–282 (2006).
7. Fagarasan, S., Kawamoto, S., Kanagawa, O. & Suzuki, K. Adaptive immune regulation in the gut: T cell-dependent and T cell-independent IgA synthesis. *Annu. Rev. Immunol.* **28,** 243–273 (2010).
8. Hayakawa, K., Hardy, R. R. & Herzenberg, L. A. Progenitors for Ly-1 B cells are distinct from progenitors for other B cells. *J. Exp. Med.* **161,** 1554–1568 (1985).
9. Kantor, A. B. & Herzenberg, L. A. Origin of murine B cell lineages. *Annu. Rev. Immunol.* **11,** 501–538 (1993).
10. Montecino-Rodriguez, E., Leathers, H. & Dorshkind, K. Identification of a B-1 B cell-specified progenitor. *Nat. Immunol.* **7,** 293–301 (2006).
11. Kunisawa, J. *et al.* Sphingosine 1-phosphate regulates peritoneal B-cell trafficking for subsequent intestinal IgA production. *Blood* **109,** 3749–3756 (2007).
12. Tsuji, M. *et al.* Requirement for lymphoid tissue-inducer cells in isolated follicle formation and T cell-independent immunoglobulin A generation in the gut. *Immunity* **29,** 261–271 (2008).
13. Gohda, M. *et al.* Sphingosine 1-phosphate regulates the egress of IgA plasmablasts from Peyer's patches for intestinal IgA responses. *J. Immunol.* **180,** 5335–5343 (2008).
14. Mora, J. R. *et al.* Generation of gut-homing IgA-secreting B cells by intestinal dendritic cells. *Science* **314,** 1157–1160 (2006).
15. Cerutti, A., Chen, K. & Chorny, A. Immunoglobulin responses at the mucosal interface. *Annu. Rev. Immunol.* **29,** 273–293 (2011).
16. Radbruch, A. *et al.* Competence and competition: the challenge of becoming a long-lived plasma cell. *Nat. Rev. Immunol.* **6,** 741–750 (2006).
17. Weinstein, P. D. & Cebra, J. J. The preference for switching to IgA expression by Peyer's patch germinal center B cells is likely due to the intrinsic influence of their microenvironment. *J. Immunol.* **147,** 4126–4135 (1991).
18. Hamada, H. *et al.* Identification of multiple isolated lymphoid follicles on the antimesenteric wall of the mouse small intestine. *J. Immunol.* **168,** 57–64 (2002).
19. Talham, G. L., Jiang, H. Q., Bos, N. A. & Cebra, J. J. Segmented filamentous bacteria are potent stimuli of a physiologically normal state of the murine gut mucosal immune system. *Infect. Immun.* **67,** 1992–2000 (1999).
20. Cebra, J. J., Jiang, H. Q., Boiko, N. V. & Tlaskalva-Hogenova, H. The role of mucosal microbiota in the development, maintenance, and pathologies of the mucosal immune system. in *Mucosal Immunology* 3rd edn (Mestecky, J. *et al.* eds) 335–368 (Academic Press, 2005).
21. Tezuka, H. *et al.* Regulation of IgA production by naturally occurring TNF/iNOS-producing dendritic cells. *Nature* **448,** 929–933 (2007).
22. Suzuki, K. *et al.* The sensing of environmental stimuli by follicular dendritic cells promotes immunoglobulin A generation in the gut. *Immunity* **33,** 71–83 (2010).
23. Shapiro-Shelef, M. & Calame, K. Regulation of plasma-cell development. *Nat. Rev. Immunol.* **5,** 230–242 (2005).
24. Patarroyo, M. *et al.* Leukocyte-cell adhesion: a molecular process fundamental in leukocyte physiology. *Immunol. Rev.* **114,** 67–108 (1990).
25. Pabst, O. *et al.* Cutting edge: egress of newly generated plasma cells from peripheral lymph nodes depends on beta 2 integrin. *J. Immunol.* **174,** 7492–7495 (2005).
26. Kunisawa, J. & Kiyono, H. A marvel of mucosal T cells and secretory antibodies for the creation of first lines of defense. *Cell Mol. Life Sci.* **62,** 1308–1321 (2005).
27. Shroff, K. E., Meslin, K. & Cebra, J. J. Commensal enteric bacteria engender a self-limiting humoral mucosal immune response while permanently colonizing the gut. *Infect. Immun.* **63,** 3904–3913 (1995).
28. Kunisawa, J. *et al.* Lack of antigen-specific immune responses in anti-IL-7 receptor alpha chain antibody-treated Peyer's patch-null mice following intestinal immunization with microencapsulated antigen. *Eur. J. Immunol.* **32,** 2347–2355 (2002).
29. Schwartzberg, P. L., Mueller, K. L., Qi, H. & Cannons, J. L. SLAM receptors and SAP influence lymphocyte interactions, development and function. *Nat. Rev. Immunol.* **9,** 39–46 (2009).
30. Maxwell, C. A., McCarthy, J. & Turley, E. Cell-surface and mitotic-spindle RHAMM: moonlighting or dual oncogenic functions? *J. Cell Sci.* **121,** 925–932 (2008).
31. Cario, E. *et al.* Lipopolysaccharide activates distinct signaling pathways in intestinal epithelial cell lines expressing Toll-like receptors. *J. Immunol.* **164,** 966–972 (2000).
32. Griffin, D. O. & Rothstein, T. L. A small CD11b(+) human B1 cell subpopulation stimulates T cells and is expanded in lupus. *J. Exp. Med.* **208,** 2591–2598 (2011).
33. Ivanov, I. I. *et al.* Induction of intestinal Th17 cells by segmented filamentous bacteria. *Cell* **139,** 485–498 (2009).
34. Hoyer, B. F. *et al.* Short-lived plasmablasts and long-lived plasma cells contribute to chronic humoral autoimmunity in NZB/W mice. *J. Exp. Med.* **199,** 1577–1584 (2004).
35. Pasare, C. & Medzhitov, R. Control of B-cell responses by Toll-like receptors. *Nature* **438,** 364–368 (2005).
36. Hou, B. *et al.* Selective utilization of Toll-like receptor and MyD88 signaling in B cells for enhancement of the antiviral germinal center response. *Immunity* **34,** 375–384 (2011).
37. Rousset, F. *et al.* Interleukin 10 is a potent growth and differentiation factor for activated human B lymphocytes. *Proc. Natl Acad. Sci. USA* **89,** 1890–1893 (1992).
38. Defrance, T. *et al.* Interleukin 10 and transforming growth factor beta cooperate to induce anti-CD40-activated naive human B cells to secrete immunoglobulin A. *J. Exp. Med.* **175,** 671–682 (1992).
39. Punnonen, J. *et al.* Soluble and membrane-bound forms of signaling lymphocytic activation molecule (SLAM) induce proliferation and Ig synthesis by activated human B lymphocytes. *J. Exp. Med.* **185,** 993–1004 (1997).
40. Tokoyoda, K., Hauser, A. E., Nakayama, T. & Radbruch, A. Organization of immunological memory by bone marrow stroma. *Nat. Rev. Immunol.* **10,** 193–200 (2010).
41. Fagarasan, S., Kinoshita, K., Muramatsu, M., Ikuta, K. & Honjo, T. In situ class switching and differentiation to IgA-producing cells in the gut lamina propria. *Nature* **413,** 639–643 (2001).
42. Kang, H. S. *et al.* Signaling via LTbetaR on the lamina propria stromal cells of the gut is required for IgA production. *Nat. Immunol.* **3,** 576–582 (2002).
43. Rakoff-Nahoum, S., Paglino, J., Eslami-Varzaneh, F., Edberg, S. & Medzhitov, R. Recognition of commensal microflora by toll-like receptors is required for intestinal homeostasis. *Cell* **118,** 229–241 (2004).
44. Hiroi, T., Yanagita, M., Ohta, N., Sakaue, G. & Kiyono, H. IL-15 and IL-15 receptor selectively regulate differentiation of common mucosal immune system-independent B-1 cells for IgA responses. *J. Immunol.* **165,** 4329–4337 (2000).

45. Yan, M. *et al.* Identification of a receptor for BLyS demonstrates a crucial role in humoral immunity. *Nat. Immunol.* **1,** 37–41 (2000).
46. Nochi, T. *et al.* Rice-based mucosal vaccine as a global strategy for cold-chain- and needle-free vaccination. *Proc. Natl Acad. Sci. USA* **104,** 10986–10991 (2007).
47. Terahara, K. *et al.* Comprehensive gene expression profiling of Peyer's patch M cells, villous M-like cells, and intestinal epithelial cells. *J. Immunol.* **180,** 7840–7846 (2008).

Acknowledgements

This work was supported by grants from the Program for Promotion of Basic and Applied Research for Innovations in Bio-oriented Industry (BRAIN to J.K.), the Ministry of Education, Culture, Sports, Science and Technology of Japan (Grants-in-Aid for Young Scientists A (22689015 to J.K.), for Scientific Research on Innovative Areas (23116506 to J.K.), for Scientific Research S (23229004 to H.K.), for Scientific Research on Priority Area (19059003 to H.K.), for Challenging Exploratory Research (24659217 to J.K.) and for the Leading-edge Research Infrastructure Program (to J.K. and H.K.)), and the Young Researcher Overseas Visits Program for Vitalizing Brain Circulation (Japan Society for the Promotion of Science) (to J.K., H.K., Y.K. and Y.G.); grants for JSPS Fellows (021-07124 to Y.K.); and grants from the Ministry of Health and Welfare of Japan (J.K. and H.K.), the New Energy and Industrial Technology Development Organization (to H.K.), the Global Center of Excellence Program of the Center of Education and Research for Advanced Genome-based Medicine (to H.K.), the Yakult Bio-Science Foundation (to J.K.) and DK085329 from the National Institute of Diabetes and Digestive and Kidney Diseases (NIDDK, to I.I.).

Author contributions

J.K. planned the research and experiments, analysed data, wrote the paper and directed the research; M.G., E.H., I.I., M.H., Y.S., Y.G., C.P., I.I.I., R.S., L.A., T.W., S.S., Y.K. and S.S. conducted the immunological experiments; K.T. and S.A. provided key materials; and H.K. wrote the paper.

Additional information

Accession codes: Microarray data have been deposited in the National Center for Biotechnology Information Gene Expression Omnibus database under series accession code GSE37225.

Supplementary Information accompanies this paper at http://www.nature.com/naturecommunications

Competing financial interests: The authors declare no competing financial interests.

Reprints and permission information is available online at http://npg.nature.com/reprintsandpermissions/

How to cite this article: Kunisawa, J. *et al.* Microbe-dependent CD11b$^+$ IgA$^+$ plasma cells mediate robust early-phase intestinal IgA responses in mice. *Nat. Commun.* 4:1772 doi: 10.1038/ncomms2718 (2013).

Infection and Immunity

Nanogel-Based PspA Intranasal Vaccine Prevents Invasive Disease and Nasal Colonization by Streptococcus pneumoniae

Il Gyu Kong, Ayuko Sato, Yoshikazu Yuki, Tomonori Nochi, Haruko Takahashi, Shinichi Sawada, Mio Mejima, Shiho Kurokawa, Kazunari Okada, Shintaro Sato, David E. Briles, Jun Kunisawa, Yusuke Inoue, Masafumi Yamamoto, Kazunari Akiyoshi and Hiroshi Kiyono

Infect. Immun. **2013, 81(5):1625. DOI: 10.1128/IAI.00240-13.**
Published Ahead of Print 4 March 2013.

IAI
Journals.ASM.org

Nanogel-Based PspA Intranasal Vaccine Prevents Invasive Disease and Nasal Colonization by *Streptococcus pneumoniae*

Il Gyu Kong,[a,b,c] Ayuko Sato,[a,d] Yoshikazu Yuki,[a,d] Tomonori Nochi,[e] Haruko Takahashi,[f] Shinichi Sawada,[f] Mio Mejima,[a] Shiho Kurokawa,[a] Kazunari Okada,[a,d] Shintaro Sato,[a,d] David E. Briles,[g] Jun Kunisawa,[a,d,h,i] Yusuke Inoue,[j] Masafumi Yamamoto,[k] Kazunari Akiyoshi,[f] Hiroshi Kiyono[a,b,d,h]

Division of Mucosal Immunology, Department of Microbiology and Immunology,[a] and International Research and Development Center for Mucosal Vaccines,[h] The Institute of Medical Science, The University of Tokyo, Tokyo, Japan; Graduate School Medicine and Faculty of Medicine, The University of Tokyo, Tokyo, Japan[b]; Department of Otorhinolaryngology, Seoul National University College of Medicine, Seoul, South Korea[c]; Core Research for Evolutional Science and Technology (CREST), Japan Science and Technology Agency, Tokyo, Japan[d]; Division of Infectious Diseases, Center for AIDS Research, University of North Carolina School of Medicine, Chapel Hill, North Carolina, USA[e]; Department of Polymer Chemistry, Kyoto University Graduate School of Engineering, Kyoto, Japan[f]; Department of Microbiology, University of Alabama at Birmingham, Birmingham, Alabama, USA[g]; Laboratory of Vaccine Materials, National Institute of Biomedical Innovation, Osaka, Japan[i]; Department of Diagnostic Radiology, Kitasato University School of Medicine, Kanagawa, Japan[j]; Department of Microbiology and Immunology, Nihon University School of Dentistry at Matsudo, Chiba, Japan[k]

To establish a safer and more effective vaccine against pneumococcal respiratory infections, current knowledge regarding the antigens common among pneumococcal strains and improvements to the system for delivering these antigens across the mucosal barrier must be integrated. We developed a pneumococcal vaccine that combines the advantages of pneumococcal surface protein A (PspA) with a nontoxic intranasal vaccine delivery system based on a nanometer-sized hydrogel (nanogel) consisting of a cationic cholesteryl group-bearing pullulan (cCHP). The efficacy of the nanogel-based PspA nasal vaccine (cCHP-PspA) was tested in murine pneumococcal airway infection models. Intranasal vaccination with cCHP-PspA provided protective immunity against lethal challenge with *Streptococcus pneumoniae* Xen10, reduced colonization and invasion by bacteria in the upper and lower respiratory tracts, and induced systemic and nasal mucosal Th17 responses, high levels of PspA-specific serum immunoglobulin G (IgG), and nasal and bronchial IgA antibody responses. Moreover, there was no sign of PspA delivery by nanogel to either the olfactory bulbs or the central nervous system after intranasal administration. These results demonstrate the effectiveness and safety of the nanogel-based PspA nasal vaccine system as a universal mucosal vaccine against pneumococcal respiratory infection.

The use of polysaccharide-based injectable multivalent pneumococcal conjugate vaccines (PCV7, -10, and -13) has diminished the number of fatal infections due to pneumococci expressing the particular polysaccharides present in the vaccine (1–3). However, *Streptococcus pneumoniae* remains a problematic pathogen (4, 5) because of the large number of different capsular polysaccharides associated with virulent disease in humans. In particular, nonvaccine strains are emerging pathogens that result in morbidity and mortality due to pneumococcal diseases, including pneumonia and meningitis (6–8).

Clinical demand to overcome these problems has prompted the preclinical development of universal serotype-independent pneumococcal vaccines that are based on a surface protein common to all strains. Pneumococcal surface protein A (PspA), a pneumococcal virulence factor (9–13), is genetically variable (14) but highly cross-reactive (9, 10). PspA is commonly expressed by all capsular serotypes of *S. pneumoniae* (15) and is classified into 3 families (family 1, clades 1 and 2; family 2, clades 3 through 5; and family 3, clade 6) according to sequence similarities (14). Given that parenteral immunization with PspA induces cross-reactive neutralizing immune responses in mice (16–18) and humans (19), using PspA as a serotype-independent common antigen for the development of pneumococcal vaccines seems to be an ideal strategy.

Pneumococcal infection is generally preceded by colonization of the upper airway (20, 21). Nasal carriage of pneumococci is the primary source for spread of the infection among humans (22, 23). Therefore, an optimal vaccine strategy to prevent and control the spread of pneumococcal disease would induce protective immunity against both colonization and invasive disease. Several studies have confirmed the efficacy of PspA as a nasal vaccine antigen by coadministering PspA with a mucosal adjuvant such as cholera toxin (CT) or cholera toxin subunit B (CTB) to mice (24–26). The mice subsequently mount antigen-specific immune responses in not only the systemic compartment but also the respiratory mucosal compartment (24, 25, 27), where bacterial colonization occurs (20). PspA-specific secretory immunoglobulin A (sIgA) antibodies induced by intranasal immunization with PspA and an adjuvant (i.e., a plasmid expressing Flt3 ligand cDNA) provide protection against pneumococcal colonization (28). In addition, studies in mice have revealed that this protection is mediated by antigen-specific interleukin 17A (IL-17A)-secret-

Received 20 February 2013 **Accepted** 21 February 2013
Published ahead of print 4 March 2013
Editor: R. P. Morrison
Address correspondence to Hiroshi Kiyono, kiyono@ims.u-tokyo.ac.jp, or Yoshikazu Yuki, yukiy@ims.u-tokyo.ac.jp.
Supplemental material for this article may be found at http://dx.doi.org/10.1128/IAI.00240-13.

doi:10.1128/IAI.00240-13

ing $CD4^+$ T cells induced by intranasal immunization with pneumococcal whole-cell antigen (29, 30).

Therefore, the intranasal vaccination route is an improved route for preventing colonization of the nasal cavity by pneumococci. A leading obstacle to the practical use of nasal vaccine with a protein-based pneumococcal antigen is the need to coadminister a toxin-based mucosal adjuvant (e.g., CT) for effective induction of antigen-specific immune responses (31, 32). However, the use of such toxin-based adjuvants is undesirable in humans, as it carries the concern that the toxin may reach the central nervous system (CNS) or redirect the vaccine antigen into the CNS through the olfactory nerve in the nasal cavity (33, 34). To bypass these concerns, we recently developed a nasal vaccine delivery system based on a non-toxin-based mucosal antigen carrier, a cationic cholesteryl pullulan (cCHP) nanogel (35).

Here we show the efficacy of a nanogel-based nasal pneumococcal vaccine in which PspA is incorporated into a cCHP nanogel (cCHP-PspA). We also characterized the cCHP-PspA-induced PspA-specific Th17 and antibody responses against *S. pneumoniae*. Mice immunized with nasal cCHP-PspA were protected from lethal challenge with *S. pneumoniae* and had fewer pneumococci on their respiratory mucosae. These results suggest that a nontoxic nasal vaccine comprising nanogel-based PspA offers a practical and effective strategy against pneumococcal infection by preventing both nasal colonization and invasive diseases.

MATERIALS AND METHODS

Mice. Female BALB/c mice (aged 6 to 7 weeks) were purchased from SLC (Shizuoka, Japan). All of the mice were housed with *ad libitum* food and water on a standard 12-h–12-h light-dark cycle. All experiments were performed in accordance with the guidelines provided by the Animal Care and Use committees of the University of Tokyo and were approved by the Animal Committee of the Institute of Medical Science of the University of Tokyo.

Recombinant PspA. Recombinant PspA of *S. pneumoniae* Rx1, which belongs to PspA family 1, clade 2 (14), was prepared as described previously, with slight modifications (26). Briefly, a plasmid encoding PspA/Rx1 (pUAB055; amino acids 1 through 302) (GenBank accession no. M74122) was used to transform *Escherichia coli* BL21(DE3) cells. This construct contains amino acids 1 through 302 of the PspA protein from strain Rx1 plus a 6×His tag at the C terminus (26). The sonicated cell supernatant was loaded onto a DEAE-Sepharose column (BD Healthcare, Piscataway, NJ) and a nickel affinity column (Qiagen, Valencia, CA). This was followed by gel filtration on a Sephadex G-100 column (BD Healthcare).

Preparation of cCHP-recombinant PspA complex for intranasal vaccination. A cCHP nanogel (size, ~40 nm) generated from a cationic cholesteryl group-bearing pullulan was used for all experiments. The cCHP-PspA complex for each immunization was prepared by mixing 7.5 μg PspA with cCHP at a 3:1 molecular ratio (volume, 18 μl per mouse) and incubating the mixture for 1 h at 45°C. Before the complex was used in *in vivo* studies, the fluorescence resonance energy transfer (FRET) of fluorescein isothiocyanate (FITC)-PspA and a tetramethyl rhodamine isothiocyanate (TRITC)-cCHP nanogel was measured with a fluorescence spectrometer (model FP-6500; Jasco, Easton, MD) as described previously (37). FRET analyses confirmed that the cCHP nanogel appropriately formed nanoparticles after the incorporation of PspA (see Fig. S1 in the supplemental material). Dynamic light scattering analysis showed that the cCHP nanogel maintained the same nanoscale size (32.8 ± 0.2 nm) even after the incorporation of PspA. Lipopolysaccharide (LPS) contamination of purified PspA and cCHP (<10 endotoxin units/mg protein) was measured with a *Limulus* test (Wako, Osaka, Japan).

Immunization. Once weekly for 3 consecutive weeks, female BALB/c mice were immunized intranasally with cCHP-PspA, PspA plus CT (1 μg; List Biological Laboratory, Campbell, CA), PspA alone, or phosphate-buffered saline (PBS) only. Some experiments included an irrelevant antigen as a control; in these studies, mice were immunized intranasally with a complex of cCHP nanogel and a recombinant nontoxic receptor-binding fragment of *Clostridium botulinum* type A neurotoxin subunit antigen Hc (cCHP-BoHc/A) (35). Serum, nasal wash fluid (NW), and bronchoalveolar lavage fluid (BALF) samples were harvested 1 week after the last immunization. For NWs, 200 μl sterile PBS was flushed through the posterior choanae (38). BALF was harvested by instilling 1 ml of sterile PBS through a blunt needle placed in the trachea (38).

Bacterial strain. We used the kanamycin-resistant pneumococcal strain *S. pneumoniae* Xen10 (Caliper Life Sciences, MA), derived from the wild-type strain A66.1, which expresses PspA of family 1, clades 1 and 2 (39). *S. pneumoniae* Xen10 carries a stable copy of the modified *Photorhabdus luminescens lux* operon at a single integration site on the bacterial chromosome (40). The virulence of *S. pneumoniae* Xen10 is comparable to that of the parent strain (40, 41). For challenge studies, *S. pneumoniae* 3JYP3670, which expresses PspA of family 2, clade 4, was used (10). All of the *S. pneumoniae* strains were grown in brain heart infusion (BHI) broth at 37°C in 5% CO_2.

Pneumococcal infection model. To evaluate the efficacy of intranasal vaccination with cCHP-PspA, mice were challenged 1 week after the last immunization. The cell densities of exponentially growing *S. pneumoniae* Xen10 cultured at 37°C in BHI broth were estimated from the optical density at 600 nm (OD_{600}); cells were pelleted and then diluted with PBS. Lethal (2×10^5 CFU) and sublethal (2×10^4 CFU) challenge doses diluted in 50 μl sterile PBS were administered intranasally to isoflurane-anesthetized mice. Mice were restrained vertically for 5 min to ensure inhalation of the organisms into the trachea. In addition, mice were inoculated intranasally with a lethal challenge dose (5×10^4 CFU) of strain 3JYP3670 in the same way as that for strain Xen10. Nasal passages and lung tissues were homogenized in 500 μl sterile PBS for 1 min, and the numbers of bacterial colonies were determined by plating samples on LB agar plates containing kanamycin (200 μl/ml).

***In vivo* imaging of immunized and challenged mice.** Bioluminescence of bacteria was monitored for 1 min 24, 48, and 72 h after lethal challenge by using an Ivis charge-coupled device (CCD) camera (Xenogen, Alameda, CA). Total photon emission from the entire thorax of each mouse was quantified by using the LivingImage software package (Xenogen). The results are provided as numbers of photons/s/cm^2/sr.

Antibody titer and subclass analysis. Antibody titers were determined by using enzyme-linked immunosorbent assay (ELISA) as described previously, with slight modifications (25). In brief, samples (2-fold serial dilutions) were loaded into individual wells, and the plate was coated with 1 μg/ml recombinant PspA and incubated. Goat anti-mouse IgA, IgG, IgG1, IgG2a, IgG2b, IgG3, and IgM (dilution factor, 1:4,000) conjugated with horseradish peroxidase were used as secondary antibodies. Reactions were visualized by using the TMB microwell peroxidase substrate system (XPL, Gaithersburg, MD). The endpoint titer is expressed as the reciprocal $\log_2$ of the last dilution that gave an OD_{450} that was 0.1 unit greater than that of the negative control.

PspA-specific $CD4^+$ T cell responses. By using anti-CD4 microbeads (Miltenyi Biotec, Sunnyvale, CA) according to the manufacturer's instructions, $CD4^+$ T cells were isolated from the spleens and cervical lymph nodes (CLNs) of mice intranasally immunized with cCHP-PspA, PspA alone, or PBS only. The purified $CD4^+$ T cells were resuspended at 1×10^6 cells/ml in RPMI 1640 (Cellgro, Mediatech, Washington, DC) supplemented with 10 mM HEPES, 50 μM 2-mercaptoethanol, 100 U/ml penicillin, 100 μl/ml streptomycin, and 10% fetal calf serum and then cocultured with irradiated (2,000 rad) splenic antigen-presenting cells (2×10^6 cells/ml) from naïve BALB/c mice for 5 days at 37°C in 5% CO_2 in the presence of 1 μg/ml PspA. Cytokine levels in $CD4^+$ T cell culture supernatants were determined by using cytokine-specific DuoSet ELISA kits

(R&D Systems, Minneapolis, MN) according to the manufacturer's instructions.

Radioisotope counting assay. To trace the distribution of PspA after intranasal immunization, PspA was labeled with indium chloride (Nihon Medi-Physics, Tokyo, Japan) anhydride (Dojindo, Kumamoto, Japan) via N-terminal and ε-Lys amino groups, using diethylenetriaminepentaacetic acid as described previously (42). ^{111}In-labeled PspA was administered alone or as a complex with cCHP nanogel. The radioisotope counts in the nasal passage, olfactory bulbs, and brain 10 min and 1, 6, 12, 24, and 48 h after instillation were estimated with a γ-counter (Wizard model 1480; PerkinElmer, Waltham, MA). The results are provided as standardized uptake values (SUVs), calculated as radioisotope counts (cpm) per gram of tissue divided by the ratio of the injected dose (1×10^6 cpm) to body weight (in grams).

Flow cytometric analysis. Mice were immunized intranasally with FITC-PspA in cCHP nanogel, FITC-PspA alone, or PBS only; 6 h later, mononuclear cells were prepared from the nasal passages of each group by mechanical dissociation through 70-μm nylon mesh, as described previously (38, 43). Isolated cells were stained with phycoerythrin (PE)-Cy7-conjugated anti-CD11c (BD Bioscience) and analyzed by flow cytometry. The percentage of PspA$^+$ cells in the CD11c$^+$ fractions was calculated for each experimental group.

Data analysis. Data are expressed as means ± standard deviations (SD). Statistical analysis for most comparisons among groups was performed with Tukey's *t* test; differences were considered statistically significant when the *P* value was <0.05. For survival data, the Fisher exact test was used to compare the numbers of alive versus dead mice in the cCHP-PspA, PspA-CT, and PBS-only groups with those in the PspA-only group.

RESULTS

Intranasal vaccination with cCHP-PspA induces protective immunity against lethal challenge with *S. pneumoniae*. To evaluate whether intranasal cCHP-PspA vaccination induces protective immunity against pneumococcal challenge, we vaccinated mice with cCHP-PspA, PspA-CT, PspA alone, or PBS only. One week after the last immunization, we lethally challenged vaccinated mice with the virulent strain *S. pneumoniae* Xen10 (2×10^5 CFU), which is *S. pneumoniae* A66.1 rendered bioluminescent by the integration of a modified *lux* operon into its chromosome (40). The PspA expression level of strain Xen10 was confirmed to be comparable to that of the parent strain (see Fig. S2 in the supplemental material). We then evaluated survival rates after lethal challenge over a 2-week period. The survival rate of the cCHP-PspA-vaccinated group was 100%, as was that for PspA-CT-vaccinated mice (Fig. 1). In contrast, most of the mice intranasally immunized with PspA alone (survival rate, 0%) or with PBS (20% survival) died within 8 days of challenge with *S. pneumoniae* Xen10 (Fig. 1). The survival rates of the groups immunized with cCHP-PspA or PspA-CT were higher and were statistically significant compared to that of the group immunized with PspA alone ($P < 0.01$). The results from the PspA-only and PBS-only groups did not differ ($P > 0.05$). In addition, immunization with the irrelevant antigen BoHc/A incorporated into cCHP (cCHP-BoHc/A) (35) did not protect mice from challenge with *S. pneumoniae* Xen10 (see Fig. S3). Because PspA family 2 (clades 3 through 5) and family 1 (clades 1 and 2) constitute 94 to 99% of clinical isolates of pneumococci (14, 44–49), we also challenged mice with the strain 3JYP3670, which expresses PspA belonging to clade 4 of family 2 (10). Unlike mice inoculated with cCHP-BoHc/A, PspA alone, or PBS only, mice nasally immunized with cCHP-PspA were protected from lethal challenge with 3JYP3670 (PspA of clade 4) (10), as was the case with Xen10 expressing PspA of clades 1 and 2 (see Fig. S4).

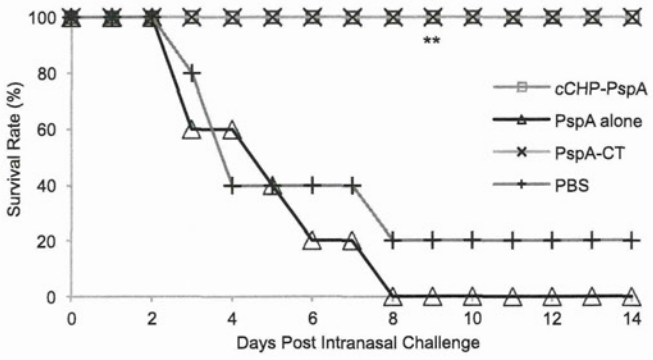

FIG 1 Intranasal vaccination with cCHP-PspA induced protective immunity against pneumococci. One week after the final immunization, mice were challenged with *S. pneumoniae* Xen10 (2×10^5 CFU/mouse), and survival was monitored. Data are representative of three independent experiments, and each group consisted of 5 mice. *P* values were calculated by using the Fisher exact test to compare the numbers of alive versus dead mice in each group with the result obtained for the PspA-only group. **, $P < 0.01$ compared with the group immunized with PspA alone. Abbreviations: cCHP, cationic cholesteryl group-bearing pullulan; CT, cholera toxin; PspA, pneumococcal surface protein A.

Intranasal vaccination with cCHP-PspA enhances bacterial clearance from BALF and the lung. To assess whether intranasal immunization with cCHP-PspA prevented pulmonary infection with pneumococci, we performed *in vivo* bioluminescence imaging of *S. pneumoniae* Xen10 after lethal challenge (2×10^5 CFU) of mice intranasally vaccinated with cCHP-PspA, PspA alone, or PBS. The lungs of mice immunized with PspA alone or with PBS only (control group) showed high-intensity photon signals in a pattern consistent with that of full-blown lung infection (Fig. 2A). In contrast, the lungs of mice immunized with cCHP-PspA lacked bioluminescence, indicating the absence of pulmonary infection. Forty-eight and 72 h after infection, photon counts of the cCHP-PspA-vaccinated group were significantly lower than those of the other two groups (Fig. 2B).

To investigate whether intranasal immunization with cCHP-PspA hastened bacterial clearance from the lung, we counted the bacteria in the BALF and lung tissues of mice intranasally vaccinated with cCHP-PspA, PspA alone, or PBS and sublethally challenged with *S. pneumoniae* Xen10 (2×10^4 CFU). Three hours after challenge, bacterial numbers in BALF (Fig. 2C) and lung tissue (Fig. 2D) did not differ among the three vaccination groups. However, 24 h after challenge, the bacterial counts in the BALF and lung homogenates from the cCHP-PspA-vaccinated groups were significantly lower (about 100-fold) than those for the mice immunized with PspA alone or PBS only (Fig. 2C and D).

Intranasal vaccination with cCHP-PspA reduces bacterial colonization in the nasal cavity. We next examined whether intranasal cCHP-PspA immunization affected nasal carriage of pneumococci in mice challenged with *S. pneumoniae* Xen10. Three days after challenge, bacterial numbers in NWs (Fig. 3A) and nasal passages (Fig. 3B) of mice immunized with the cCHP-PspA nasal vaccine were decreased significantly (approximately 100-fold) compared to those for the two control groups.

Intranasal vaccination with cCHP-PspA induces strong Th17 and Th2 responses. We then examined the type of immune

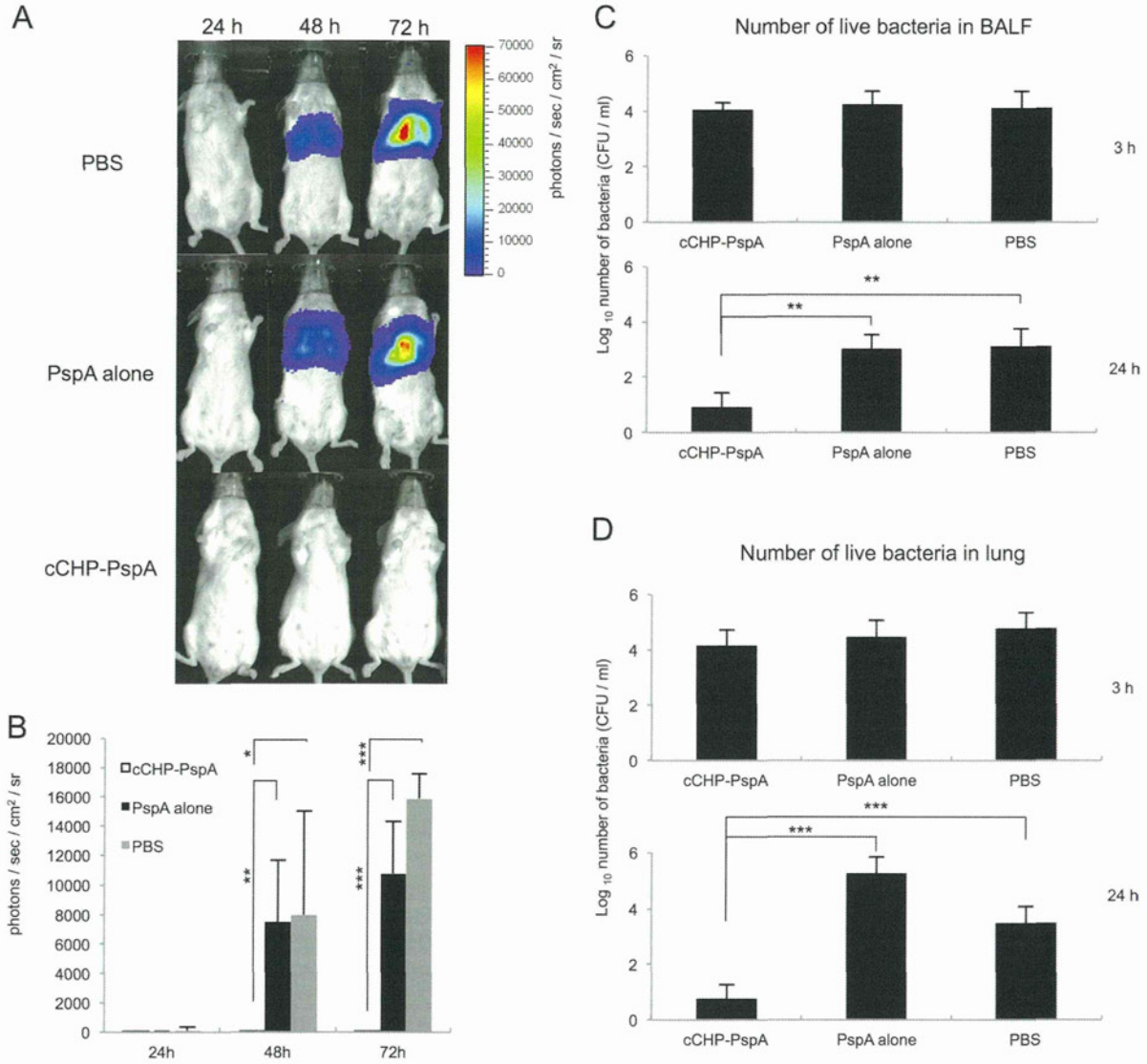

FIG 2 *In vivo* imaging revealed no sign of pneumococcal infection in the lungs of mice immunized intranasally with cCHP-PspA; these mice also showed enhanced bacterial clearance from the BALF and lung. Images (A) and average photon counts (B) show bioluminescence due to *S. pneumoniae* Xen10 in each group of mice infected intranasally with *S. pneumoniae* Xen10 (2×10^5 CFU/mouse) and imaged 24, 48, and 72 h after infection. (C and D) One week after the final immunization, mice were challenged with a sublethal dose (2×10^4 CFU/mouse) of *S. pneumoniae* Xen10. BALF and lung tissues were collected, and the numbers of *S. pneumoniae* Xen10 organisms 3 and 24 h after challenge were determined. Data are representative of three independent experiments, and each group consisted of 5 mice. *, $P < 0.05$; **, $P < 0.01$; ***, $P < 0.001$. Abbreviations: BALF, bronchoalveolar lavage fluid; cCHP, cationic cholesteryl-group-bearing pullulan; PspA, pneumococcal surface protein A.

responses elicited by intranasal cCHP-PspA vaccination. Compared with PspA alone or PBS, cCHP-PspA induced higher levels of IL-17 in $CD4^+$ T cells from the spleen, CLNs, and nasal passages (Fig. 4A). The cCHP-PspA-vaccinated group produced high levels of IL-4 and IL-13, the hallmark cytokines of a Th2-type immune response, but only scant amounts of gamma interferon (Fig. 4B to D). These results show the potential of a cCHP-PspA nasal vaccine as an advanced pneumococcal vaccine that can induce a Th17 response together with a Th2-type immune response.

Intranasal vaccination with cCHP-PspA induces high levels of systemic antibodies. To address whether intranasal administration of cCHP-PspA induced PspA-specific antibody responses, we examined the serum titers of PspA-specific antibodies. PspA-specific IgG responses in the systemic compartment were significantly higher in mice immunized with intranasal cCHP-PspA than in those given PspA only (Fig. 5A). Unlike the predominant IgG response, IgM and IgA titers in the serum samples were very low (Fig. 5A).

Intranasal immunization with cCHP-PspA induced primarily IgG1 antibodies, followed by IgG2b antibodies (Fig. 5B). This pattern indicated skewing toward a Th2-type response and was consistent with the cytokine profiles of the culture supernatants from antigen-stimulated $CD4^+$ T cells prepared from the same mice (Fig. 4B and C).

Intranasal vaccination with cCHP-PspA induces high levels of mucosal antigen-specific sIgA antibodies. We next examined whether vaccinated mice also produced mucosal antigen-specific Ig responses. Intranasal vaccination with cCHP-PspA induced